

13

15

16

17

18

19

20

21

22

23

24

25

26

27



- Retrieving root-zone soil moisture from land surface modelling and
- 2 GRACE/-FO and validating its dynamics with in-situ data over West

3 Africa

- Loudi Yap^{1,2}, Jürgen Kusche², Bamidele Oloruntoba^{3,4}, Helena Gerdener², and Harrie-Jan
- Hendricks Franssen^{3,4}
- ¹Research Laboratory in Geodesy, National Institute of Cartography, Cameroon
- ²Institute of Geodesy and Geoinformation (IGG), University of Bonn, Germany
- ³Institute of Bio- and Geosciences: Agrosphere (IBG-3), Forschungszentrum Jülich GmbH,
- 52425 Jülich, Germany
- ⁴Centre for High-Performance Scientific Computing in Terrestrial Systems, Geoverbund
- ABC/J, 52425 Jülich, Germany.
- Corresponding author: L. Yap. E-mail addresses:loudiyap@uni-bonn.de, loudiyap@yahoo.fr.

14 Abstract

Rainfall variability in West Africa, driven by the West African Monsoon, poses significant challenges to agricultural productivity and livelihoods. In this context, understanding root-zone soil moisture (RZSM) dynamics is crucial since it serves as the primary water source for crops. While surface soil moisture (SSM) has been widely studied, research on RZSM remains limited. This study investigates RZSM dynamics across West Africa from 2003 to 2019 using multiple satellitederived and model-based datasets, including ESA CCI v0.81, GLWS2.0, WaterGAP, CLM5.0, and in-situ observations. Results indicate that ESA CCI exhibits the strongest temporal and spatial alignment with ground measurements, whereas CLM5.0 and GLWS2.0 effectively capture latitudinal soil moisture gradients associated with climatic zones. A novel application of an analytical solution to Richards' equation was employed to translate surface moisture signals to deeper soil layers, demonstrating GLWS2.0's superior ability to reproduce seasonal patterns at various depths, notably in Benin and Niger. Despite challenges posed by sparse in-situ data and vegetation-induced signal attenuation, the study highlights the significant benefits of GRACE/-FO data assimilation





- in enhancing model accuracy. The proposed depth-projection methodology improves the vertical
- 29 representation of soil moisture, offering new insights into the dynamics of surface and subsurface
- 30 water storage. These findings have important implications for agricultural forecasting, sustain-
- able water resource management, and climate adaptation strategies in regions where accurate soil
- moisture data are essential for resilience planning.

33 Keywords

- 34 West Africa, Root-zone soil moisture, Satellite-derived soil moisture, Richards' equation, GRACE/-FO
- 35 data assimilation

36 Highlights

- Comprehensive assessment of root-zone soil moisture (RZSM) dynamics across West Africa
 (2003–2019) using multiple satellite- and model-based datasets.
- Novel depth-projection approach based on Richards' equation translates surface soil moisture signals to deeper layers, enhancing geodetic representation of subsurface water storage.
- ESA CCI shows the strongest temporal alignment with in-situ observations, while GLWS2.0 and CLM5.0 capture latitudinal and seasonal SM patterns effectively.
- Integration of GRACE/-FO satellite gravimetry improves GLWS2.0 accuracy, supporting geodeticbased monitoring of water resources and hydrological forecasting.
- Methodological framework advances understanding of surface and subsurface water mass redistri-
- bution, contributing to geodesy-informed sustainable water management and climate adaptation
- strategies.





48 1 Introduction

Rainfall in West Africa is largely driven by the West African Monsoon (WAM), characterized by significant spatial and temporal variability (Diatta & Fink, 2014). This variability, often sporadic and unpredictable, increases the region's vulnerability to droughts and floods, severely impacting agricultural productivity and leading to crop failures in rainfed systems (Sonwa et al., 2017; Galle et al., 2018; Myeni et al., 2019). As a result, smallholder farmers, reliant on rainfed agriculture and constrained by financial limitations, face heightened risks to their livelihoods (IPCC, 2023). These challenges significantly hinder economic development and exacerbate poverty in this already vulnerable region, which relies on agriculture for the livelihoods of around 70% of its estimated 420 million people, with a rapidly growing population at an annual rate of 2.2 - 2.8% (UN Department of Economic and Social Affairs, 2020). Root-zone soil moisture (RZSM) which refers to the amount of water stored in the soil within the root zone of vegetation, typically the top 1-2 meters serve as the primary water source for crops (Helman et al., 2019). RZSM directly influences plant growth, agricultural productivity, and water availability for ecosystems (Pegram et al., 2010; Seneviratne et al., 2010; Chartzoulakis & Bertaki, 2015; Helman et al., 2019). Unlike surface soil moisture (SSM), which can quickly change due to weather conditions, RZSM represents the longer-term water storage available to plants, playing a key role in determining drought resilience and crop yields (Chartzoulakis & Bertaki, 2015). Given that approximately 75% of the total crop area harvested globally consists of non-irrigated crops (Portmann et al., 2010; Grillakis et al., 2021), the importance of RZSM in global food production and food security becomes even more pronounced. Monitoring RZSM is essential for understanding the water balance (Koster et al., 2004), drought and flood warning (Gavahi et al., 2020; Watson et al., 2022), managing irrigation (Rodríguez-Iturbe & Porporato, 2007; Brocca et al., 2017), and modeling climate impacts on agriculture and natural vegetation (Ruichen et al., 2023). It potentially enhances forecasts and climate projections, guides water resources management, and supports precision agriculture by optimizing water usage. Currently, soil moisture products (SSM or RZSM) can be generated using three different key 73 approaches: in situ observations, remote sensing, and modelling (Brocca et al., 2017). In situ observations involve ground-based sensors that measure soil moisture directly at specific points using gravimetric, tensiometric and nuclear methods (Myeni et al., 2019). These measurements are reasonably accurate and can capture soil moisture at different depths. However, while in situ observations offer precision, they are labor-intensive and expensive to maintain, and their limited spatial coverage makes them difficult to scale across large regions (Dorigo et al., 2013). This poses challenges in using them for extensive, long-term monitoring over large areas. Nevertheless, the point-scale ground obhttps://doi.org/10.5194/egusphere-2025-4600 Preprint. Discussion started: 14 October 2025 © Author(s) 2025. CC BY 4.0 License.





servations are often used as a benchmark for calibrating and validating soil moisture estimates from remote sensing and model simulations (Su et al., 2014; Brocca et al., 2017; Myeni et al., 2019). In recent years, significant efforts have been made to establish in situ soil moisture monitoring networks across Africa, particularly exemplified by the AMMA-CATCH (African Monsoon Multi-disciplinary Analysis-Couplage de l'Atmosphère Tropicale et du Cycle Hydrologique) observatory (Galle et al., 2018). Some of the data collected from these networks have been integrated into the International Soil Moisture Network (ISMN)(https://ismn.geo.tuwien.ac.at/) (Dorigo et al., 2013). These sparse in situ monitoring networks have played a crucial role in validating remotely sensed and simulated soil moisture estimates over extended periods in various African regions (Jung et al., 2019). Remote sensing utilizes various methods, such as microwave, optical, and thermal satellite sensors, to estimate surface soil moisture across large areas (Brocca et al., 2017; Myeni et al., 2019). It is an effective technique for detecting the dynamic patterns of soil moisture on regional and global scales. Various satellite instruments, including the Soil Moisture Active Passive (SMAP), Soil Moisture and Ocean Salinity (SMOS), METOP-A/B Advanced Scatterometer (ASCAT), Advanced Microwave Scanning Radiometer-EOS (AMSR-E), and products from the European Space Agency's Climate Change Initiative (ESA CCI), have been successfully utilized to retrieve SSM at a global scale with a temporal resolution of 2 to 3 days (Njoku et al., 2003; Bartalis et al., 2007; Kerr et al., 2012; Entekhabi et al., 2010; Dorigo et al., 2017; Montzka et al., 2017; Chen et al., 2018). While the remote sensing approach offers broad spatial coverage and frequent updates, it primarily measures soil moisture in the uppermost few centimeters (0-5 cm), often missing the deeper root zone dynamics. Additionally, its accuracy can be impacted by factors such as vegetation, weather conditions, radio frequency interference (RFI), and topography, 101 which can reduce measurement reliability. In contrast, the GRACE (Gravity Recovery and Climate 102 Experiment) mission captures changes in total water storage by mapping variations in Earth's gravity 103 field (Tapley et al., 2004). It has been demonstrated that GRACE-observed Total Water Storage 104 Anomalies (TWSA) can be translated into surface or root zone soil moisture (SSM or RZSM) using 105 a physically based approach (Grippa et al., 2011; Sadeghi et al., 2020). Although GRACE-based soil 106 moisture data have lower spatial resolution $\sim 3^{\circ}$ vs. 40 km for microwave data) and less frequent 107 temporal sampling (monthly vs. daily), data assimilation and downscaling algorithms can be applied 108 to make these two approaches comparable (Gerdener et al., 2023). Additionally, GRACE data are not 109 affected at all by vegetation density and RFI. This study will incorporate this approach. The modelled 110 data approach uses simulations that integrate climatic, soil, and vegetation information to estimate 111 both surface and root zone soil moisture across various spatial and temporal scales. Whether based on hydrological or land surface models, both approaches rely on similar equations to simulate soil





moisture according a water balance approach (Famiglietti & Wood, 1994). Modelling allows for soil moisture estimates to be generated at high spatial and temporal resolution, offering detailed insights 115 into soil moisture dynamics. However, while models provide comprehensive coverage and long-term predictions, their accuracy is highly dependent on the quality of meteorological input data and the 117 assumptions made in parameterization, which can introduce significant uncertainties. As a result, 118 each modelling approach has its strengths and limitations, and combining multiple methods can pro-119 vide a more robust and reliable understanding of soil moisture dynamics. While numerous studies have focused on monitoring remotely sensed and modeled surface soil moisture data over West Africa 121 (Pellarin et al., 2009a,b; Gruhier et al., 2010; Baup et al., 2011; Fatras et al., 2012; Louvet et al., 122 2015; Faridani et al., 2017) using in situ data, there has been little to no research, to our knowledge, 123 specifically examining root-zone soil moisture in this region. Furthermore, while the remote sensing products monitored in this area primarily involve AMSR-E satellite data (Pellarin et al., 2009a,b; 125 Gruhier et al., 2010), the SMOS satellite mission (Louvet et al., 2015; Jung et al., 2019), and ASCAT satellite data (Jung et al., 2019), soil moisture products based on ESA CCI, CLM5.0, and GRACE/-127 FO assimilated data have not been comprehensively validated in this region. However, while many physically-based land surface models (e.g., CLM5.0) simulate the soil moisture patterns at different depths by numerically solving Richard's equation, this remains a challenge for conceptual hydrological 130 models. This study aims to retrieve the root-zone soil moisture from a conceptual model, WaterGAP, 131 as well as the GRACE/-FO-based global assimilation model GLWS2.0 which is based on WaterGAP. 132 The dynamics of these estimates will be validated against in-situ measurements, while additional soil moisture products, including ESA CCI and CLM5.0, will be used for comparative analysis across the West Africa region. 135

Our main research questions are:

- 137 1. What is the correlation between the SM from the GRACE/-FO-based global assimilation model (GLWS2.0) and ESA CCI, in-situ data, and other land surface models in the region?
- 2. How can the water content in the single soil moisture reservoir from the conceptual hydrological models be translated to a soil moisture vertical profile?
- 3. How does the root-zone soil moisture (RZSM) changes at each retrieval depth over 2003–2019 in this region? What is the correlation of its dynamics with the physically-based model (CLM5.0), ESA CCI products, and in-situ data?
- The analytical solution of Richards' equation (Sadeghi et al., 2020) will be used to translate water content from the single soil moisture reservoir in GLWS2.0 and WaterGAP to different depths. Our





approach offers a distinct advantage over that of Sadeghi et al. (2020), who assumes that GRACE TWSA (Total Water Storage Anomaly) data have minimal contributions from sources such as groundwater, surface water, or lateral groundwater flow. In their case, any TWSA variation not physically attributable to soil moisture and incompatible with their model is classified as error. By contrast, we 149 work directly with the soil moisture anomaly derived from GLWS2.0 (or WaterGAP), where non-soil 150 moisture components have already been filtered out, offering a cleaner signal for analysis. However, 151 it is important to note that complete separation of these additional hydrological signals from soil moisture may still be imperfect within the assimilation or WaterGAP model. WaterGAP (and thus 153 GLWS2.0) represents soil moisture via a single layer that extends to the root zone. The model simu-154 lates varying surface water storages (lakes, wetlands, rivers, and reservoirs) and includes a conceptual 155 groundwater representation. Human water use, i.e. surface and groundwater abstractions, are in-156 cluded in WaterGAP. This approach provides a promising solution to not only expand the shallow 157 vertical support of the microwave satellites with good spatial resolution but also to better isolate the 158 groundwater storage dynamics from the GRACE/-FO-based assimilated signal. This is particularly 159 relevant in West Africa, where soil moisture has been shown to be the dominant component of Total Water Storage (TWS) (Getirana et al., 2017; Jung et al., 2019; Jensen et al., 2024).

¹⁶² 2 Study area and datasets

163 2.1 Study area

The study area encompasses West Africa, spanning from 17°W to 17°E and 2°N to 21°N (Fig. 1). The terrain in this region is predominantly low and flat (Tappan et al., 2016). The area is characterized by a latitudinal gradient that includes three bioclimatic regions, progressing from north to south: the Sahelian, Sudanian, and Guinean zones (Galle et al., 2018). This gradient results in varying vegetation 167 patterns (Fig.2), with the arid north experiencing a single rainy season and sparse vegetation, while 168 the south has two rainy seasons and dense vegetation (Fink et al., 2010). Three meso-scale sites located at different latitudes in Benin, Niger, and Senegal, where AMMA SM observations have undergone advanced quality control procedures by the ISMN, have been selected for analysis in this 171 study (Fig. 1). The Benin site, situated in the Sudanian climate zone, features sandy clay loam soils, woody savanna vegetation, and gently undulating topography (630–225 m asl), with about 1200 mm of annual rainfall concentrated in a single rainy season from April to October (Galle et al., 2018). Both the Niger and Senegal sites are located in the Sahel region characterized by a single rainy season between June and October. The Niger site experiences a semi-arid tropical climate, characterized by





a long dry season from October to May, with an average yearly temperature of 29.2°C and 520 mm of annual rainfall (1990–2007)(Galle et al., 2018). The landscape features flat lateritic plateaus and sandy valleys within the Iullemmeden sedimentary basin, which has endorheic hydrology and a continental terminal aquifer. Soils are sandy and weakly structured, contributing to erosion. Additionally, the original woody savannah has transformed into a mosaic of rainfed millet fields and shrubby savannah, mixed with degraded tiger bush vegetation (Cappelaere et al., 2009). The Senegal site, situated in the Dahra region (15.432°W – 15.403°N), has a Sahelian climate with a mean yearly temperature of 29°C, peaking in May, and an annual precipitation of approximately 420 mm. The area features herbaceous vegetation dominated by annual grasses and a tree cover of about 3%, with most water bodies being temporary, except for a few permanent ponds (Soti et al., 2010; Guilloteau et al., 2014).

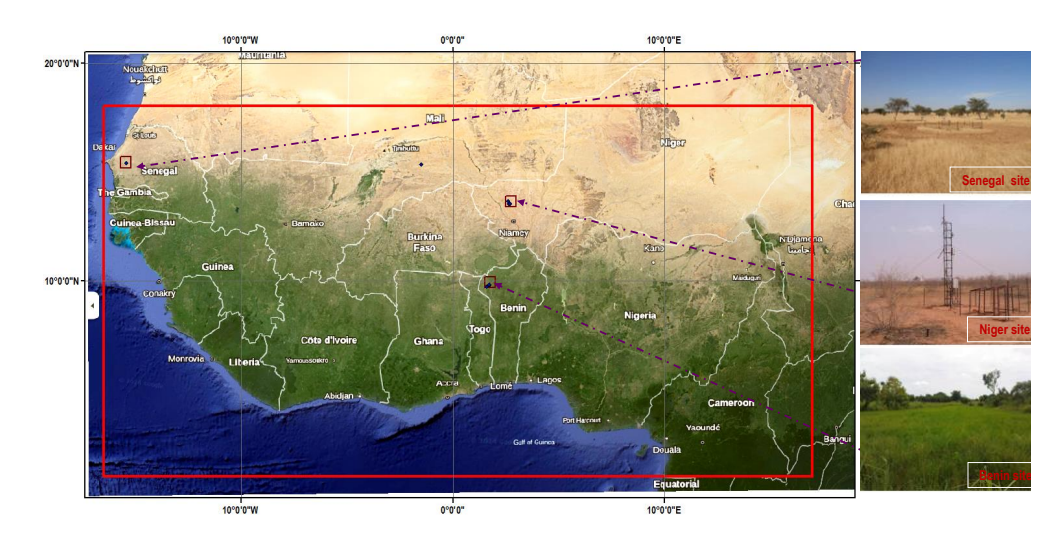


Figure 1: Location of the three meso-scale sites in Benin, Niger, and Senegal where in situ SM stations are installed. Purple boxes of 0.5° pixel of size include the in situ soil moisture stations illustrated with green dots (04 for Benin site, 03 for Niger site, and 01 for Senegal site). The red rectangular region is where the grid validation (ESA CCI versus CLM5.0, GLWS2.0 and WaterGap) is done. Photos used in this figure are adapted from (Louvet et al., 2015)

Page 2.2 Datasets

88 2.2.1 WaterGAP and GLWS2.0

This study utilizes version 2.2e of the WaterGAP global hydrology model (Müller Schmied et al., 2021), which simulates daily water fluxes and storage on a 0.5° grid by solving water balance equations across ten water compartments. These compartments represent different storage components within the hydrological cycle, including surface water (rivers, lakes, reservoirs, wetlands), soil mois-





ture, groundwater, snow, glaciers, canopy water, and river floodplains. The model's vertical water balance includes components such as the canopy, snow, and soil moisture, while the lateral water 194 balance accounts for storage in groundwater, lakes, artificial reservoirs, wetlands, and rivers. The vertical water balance is expressed in terms of water height (measured in millimeters), whereas the 196 lateral water balance is calculated using volumetric units (in cubic meters) (Müller Schmied et al., 197 2021). Unlike many land surface models, WaterGAP incorporates human water use for various pur-198 poses, including irrigation, livestock, industry, domestic consumption, and cooling of thermal power plants, and is calibrated against long-term annual river discharge. A significant update in this ver-200 sion is the enhanced algorithm for surface and groundwater abstraction. The model employs forcing 201 data from the homogenized GSWP3-W5E5 reanalysis dataset, which includes precipitation, temper-202 ature, long-wave radiation, and shortwave radiation (Lange et al., 2022), as well as information on the characteristics of surface water bodies (lakes, reservoirs, and wetlands), land cover, soil type, 204 topography, and irrigated areas. Since its inception in 1996, WaterGAP has been instrumental in 205 assessing the dynamic development of the human-water system, both historically and into the future, 206 particularly in the context of climate change. The model has significantly improved our understanding 207 of changes in continental water storage, with a particular emphasis on the overuse and depletion of water resources (Müller Schmied et al., 2021). GLWS 2.0, or the Global Land Water Storage dataset 209 version 2.0, is developed by assimilating monthly Total Water Storage Anomaly (TWSA) maps from 210 GRACE and GRACE-FO into the WaterGAP global hydrological model. The Ensemble Kalman Filter (EnKF) (Evensen, 2003) was used for assimilation, which is implemented through the Parallel Data Assimilation Framework (PDAF) (Nerger & Hiller, 2013). The assimilation process includes 213 vertical disaggregation to optimally combine GRACE/GRACE-FO data with inputs from the hy-214 drological model, resulting in ten distinct water compartments. GLWS 2.0 covers global land areas, 215 excluding Greenland and Antarctica, with a spatial resolution of 0.5° and spans the period from 2003 to 2019, ensuring no gaps in the data. It also incorporates monthly uncertainty quantification at the 217 grid cell level. Key improvements in GLWS 2.0 compared to its predecessor, GLWS 1.0, include the 218 integration of the updated WaterGAP version 2.2e and minor bug fixes in the assimilation process. 219 Comprehensive details about the development of GLWS 2.0 can be found in Gerdener et al. (2023).

221 2.2.2 CLM5.0

In this study, we use CLM5.0, the latest version of the Community Land Model (CLM), which operates in land-only mode over the CORDEX-Africa domain (Bayat et al., 2023; ?). This configuration uses atmospheric reanalysis datasets as external forcings rather than coupling CLM5.0 with an atmospheric





model. CLM5.0 simulates key biophysical and biogeochemical processes, such as the interaction between incoming radiation and the canopy/soil, and the exchange of sensible heat, latent heat, and 226 carbon with the atmosphere (Lawrence et al., 2019). Additionally, the model incorporates snow accumulation and melting, along with water and energy transport in the soil. It captures processes such 228 as infiltration, surface runoff, deep percolation, stomatal physiology, and photosynthesis. To account 229 for land surface variability, CLM5.0 divides each grid cell into multiple land units with unique soil or 230 snow columns and plant functional types (PFTs), allowing for a more nuanced representation of surface heterogeneity (Lawrence et al., 2019). Compared to earlier versions like CLM4.5, CLM5.0 provides 232 enhanced accuracy in simulating hydrological and ecological processes and introduces a more explicit 233 representation of human land management, making it a powerful tool for analyzing land-atmosphere 234 interactions and land-use impacts (Lawrence et al., 2019). The model relies on a comprehensive set of atmospheric forcing data, including precipitation, air temperature, shortwave and longwave radiation, 236 specific humidity, surface air pressure, and wind speed. This data is available at different temporal 237 resolutions: every 6 hours for CRUNCEP, every 3 hours for GSWP, and hourly for WFDE5. It oper-238 ates at a high horizontal resolution of approximately 0.027° (around 3 km) with a 30-minute time step, 239 and output data are further aggregated to a monthly scale for the analysis. Soil moisture in CLM5.0 is expressed in volumetric units (cm³/cm³) for each soil layer, structured through a 25-layer soil model 241 extending to a depth of 42 meters. Of these, 20 layers are hydrologically and biogeochemically ac-242 tive, providing the simulation of vertical soil moisture transport through the numerical solution of the Richards equation (Zeng & Decker, 2009). This layered approach improves the model's capacity to capture the vertical distribution of water in the soil, critical for understanding root-zone hydrological processes. For further details on CLM5.0's methods for simulating processes, surface characterization, and vertical soil discretization, refer to Lawrence et al. (2019) and Oloruntoba et al. (2025).

2.2.3 In-situ soil moisture data

Soil moisture observations from three meso-scale sites in Benin, Niger, and Senegal (Figure 1) spanning from 2003 to 2019 were sourced from the International Soil Moisture Network (ISMN) (Dorigo et al., 2011) to evaluate the accuracy of model-simulated soil moisture in both surface soil moisture (SSM) and root zone soil moisture (RZSM). Table 1 details the geographical coordinates of the soil moisture stations, land-cover types, and the depths of the available soil moisture probes. The locations of the soil moisture stations within the 0.25° satellite pixels are illustrated in Figure 1. Specifically, there are four stations in Benin (Belefoungou-top, Belefoungou-middle, Nalohou-top, and Nalohou-middle), three stations in Niger (Banizoumbou, Tondikiboro, and Wankama), and one sta-





tion in Senegal (Dahra). Each soil moisture dataset includes hourly observations in volumetric units (cm³/cm³) at various depths, as outlined in Table 1. Only observations that have undergone rigorous quality control procedures and were flagged as "Good" by the ISMN, were selected for analysis (Dorigo et al., 2013). This ensures that the in-situ data used is of the highest reliability, having passed through stringent checks for accuracy, consistency, and completeness. By focusing exclusively on these high-quality observations, we aim to minimize errors and uncertainties in the results, leading to more robust and credible findings. Additional information regarding the instruments used and the data quality control procedures for the observations can be found in the network reports and the associated references, which are accessible at https://ismn.geo.tuwien.ac.at.

Table 1: Geographic coordinates, stations grouped by site, probe depths, and land-cover types where the probes are installed.

Sites	Stations	Latitude	Longitude	Probes depths (cm)	Land-cover	
Benin	Nalohou (top)	9.743° N	1.606° E	5, 10, 20, 40, 60, 100	Mixed crops	
	Nalohou (middle)	9.745° N	1.605° E	5, 10, 20, 40, 120	Mixed crops	
	Belefoungou (top)	9.790° N	1.710° E	5, 10, 20, 40, 60, 100	Forest	
	Belefoungou (middle)	9.795° N	1.715° E	5, 10, 20, 40, 50, 100	Forest	
Niger	Wankama	13.646° N	2.632° E	5, 10-40, 40-70, 70-100, 100-130	Millet	
_	Banizoumbou	13.532° N	2.660° E	5	Fallow	
	Tondikiboro	13.548° N	2.696° E	5, 10-40, 40-70, 70-100, 100-130	Fallow	
Senegal	DAHRA	15.403° N	15.432° W	5, 10, 30, 50, 100	shrubland	

265

2.2.4 ESA-CCI soil moisture

The ESA-CCI is a global satellite-observed soil moisture (SM) dataset developed under the European Space Agency's Climate Change Initiative (CCI). The ESA-CCI SM v0.81 is the latest version data 268 used in this study, providing daily estimates of global surface soil moisture, covering the top 2-269 5 cm of soil, over a long term (1978-2022) at a spatial resolution of 0.25°. The ESA-CCI SSM 270 v0.81 dataset is generated by merging SM data from 12 single-sensor active and 5 passive microwave sensors. For detailed information on the key features of these active and passive microwave sensors, 272 please refer to Gruber et al. (2020). Despite some limitations associated with the chosen merging 273 algorithm and the quality of individual data sources, the v0.81 version has shown significant promise for assessing model performance (Hirschi et al., 2023; Palagiri et al., 2024). In this study, the combined product, which integrates soil moisture retrievals from both active and passive microwave sensors, is selected, as it benefits from the strengths of both types of observations and generally outperforms products that rely solely on single-sensor input (Gruber et al., 2020; Hirschi et al., 2023). The dataset 278 is available free of charge from the ESA website and other platforms, provided in volumetric units (cm³/cm³) and in NetCDF format, making it accessible for long-term climate and hydrological studies.





A detailed description of the ESA-CCI SSM product can be found at: http://www.esa-soilmoisturecci.org/node/139.

283 **2.2.5** Land cover

The land cover data used in this study is sourced from versions v2.0.7cds and v2.1.1 of the European Space Agency's Climate Change Initiative Land Cover (ESA CCI-LC) dataset, accessed from https://www.esa-landcover-cci.org (ESA, 2024; last access: 31 August 2024). Version v2.0.7cds covers the period 1992–2015, while v2.1.1 provides data for 2016–2019. However, for this research, the version v2.0.7cds is used for the period 2003–2015, and v2.1.1 for 2016–2019.

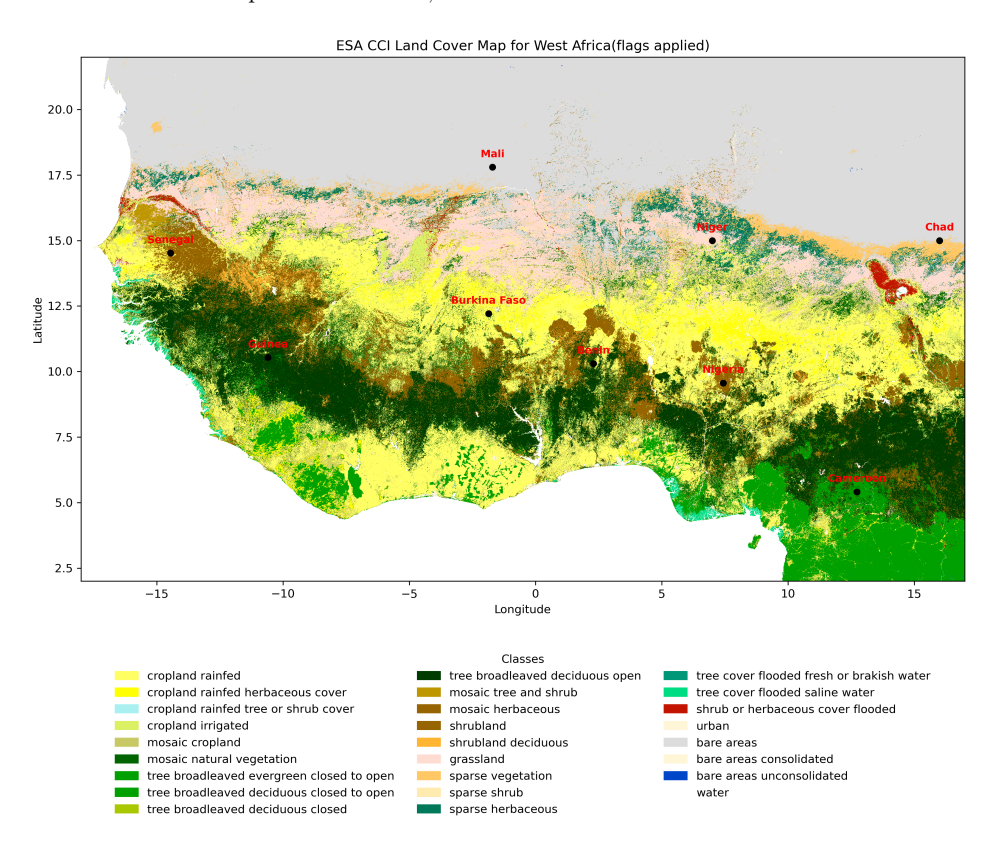


Figure 2: Land cover map over the study area.

The ESA CCI-LC dataset offers global annual land cover maps at a 300-meter spatial resolution in NetCDF format, spanning 1992 to 2019. These maps are produced by integrating observations from multiple satellite sensors (e.g., MERIS, SPOT-VGT, PROBA-V) using time-series analysis and supervised machine learning classification based on the Land Cover Classification System (LCCS) (Defourny et al., 2023). The dataset's accuracy has been validated by several studies (Defourny et al.,





²⁹⁴ 2023; Chisanga et al., 2024). The land cover map for this study (Figure 2) was generated by processing NetCDF files, clipping the data to the West Africa region, and calculating the dominant land cover class per pixel for the period 2007–2019, with key land cover types including cropland, tree cover, shrubland, grassland, urban areas, and bare areas.

298 3 Methods

The methods are organized into four main steps. The detailed procedure for retrieving root-zone soil moisture from conceptual models (GLWS2.0 and WaterGap) is outlined in Section 3.1, while the approach for assessing spatial footprint is discussed in Section 3.2. Data pre-processing procedure is covered in Section 3.3, and the performance validation approach is presented in Section 3.4.

3.1 Projecting root zone soil moisture to specific depth

An approach based on the analytical solution of Richards' equation is used to translate the water content from the single soil moisture reservoir in the conceptual hydrological models to different depths. Equation (1) below was applied to retrieve the soil moisture (SM) signal at any given depth, following the procedure outlined in (Sadeghi et al., 2020):

$$\frac{\partial \theta}{\partial t} = D \frac{\partial^2 \theta}{\partial z^2} - k \frac{\partial \theta}{\partial z} \tag{1}$$

309 Where:

311

- θ is the volumetric soil moisture content (cm³/cm³),
 - t is the time (month),
- z is the soil depth (positive downward) (cm),
- D is the effective soil water diffusivity (an average value over the entire saturation range) (cm²/month),
- k is the average slope of the soil hydraulic conductivity function, which describes the relationship between unsaturated hydraulic conductivity K (cm/month) and volumetric soil moisture θ .

The soil hydraulic parameters D and K vary with soil type and are calibrated at each site according to the methodology outlined in Sadeghi et al. (2020). The equation (1) illustrates how the soil moisture content, represented by prescribed boundary conditions, changes over time and depth due to soil water diffusion and conductivity. The closed-form solution for determining soil moisture at any arbitrary



330

332



depth during the $N^{\rm th}$ time step with time intervals of ΔT (as shown in Equation (2)) is derived by utilizing Warrick (1975) approach to solve Equation (1). This solution is developed while following the boundary and initial conditions specified in Sadeghi et al. (2020). This equation (2) is given by:

$$\theta_N(Z) = \begin{cases} \exp(-0.5Z + 0.25T)F_1U(Z,T) & \text{for } N = 1\\ \exp(-0.5Z + 0.25T)\left\{F_1U(Z,T) + \sum_{i=2}^{N} (F_i - F_{i-1})U(Z,[N-i+1]\Delta T)\right\} & \text{for } N > 1 \end{cases}$$
(2a)

$$U(Z,T) = -0.5 \exp(Z) (Z + T + 1) \operatorname{erfc} \left[0.5 \left(\frac{Z}{\sqrt{T}} + \sqrt{T} \right) \right]$$

$$+ \sqrt{\frac{T}{\pi}} \exp \left(- \left[0.5 \left(\frac{Z}{\sqrt{T}} - \sqrt{T} \right) \right]^{2} \right) + 0.5 \operatorname{erfc} \left[0.5 \left(\frac{Z}{\sqrt{T}} - \sqrt{T} \right) \right]$$
(2b)

where erfc is the complementary error function and T, Z and F are dimensionless representations of time t, soil depth z, and net water flux f given by:

$$Z = \frac{z \cdot k}{D},$$

$$T = \frac{t \cdot k^2}{D},$$

$$F = \frac{(f - k \cdot \theta_{\infty})}{(k \cdot \theta_{\infty})}.$$
(3)

A closed-form solution is obtained by assuming a stepwise surface flux input F defined as follows:

$$F(T) = \begin{cases} F_1 & \text{for } 0 < T < \Delta T \\ F_2 & \text{for } \Delta T < T < 2\Delta T \\ \vdots & & \\ F_N & \text{for } (N-1)\Delta T < T < N\Delta T \end{cases}$$

$$(4)$$

 θ_{∞} as defined in F, represents the long-term temporal mean of relative soil moisture at a given site. The implementation of this approach in our research assumes that the time derivative of the soil moisture component, derived from either the GLWS 2.0 or WaterGAP models, approximates the net water flux f as shown in Eq. (3). Central differencing is employed to avoid introducing a phase lag. This approximation yields the dimensionless flux F, which is used in Eq. (2a). The analytical formulation of Eq. (2) enables the computation of the soil moisture profile from GLWS 2.0 or WaterGAP at monthly intervals, eliminating the risk of "truncation error" that can arise in numerical solutions of Richards' equation (Zeng & Decker, 2009). The soil moisture profile at any desired depth, aligned





with the node depths of CLM5 for subsequent comparison, is calculated using Eq. (2).

42 3.2 Spatial footprint

Spatial footprint, or spatial representativeness, refers to the area surrounding a soil moisture (SM) station within which temporal soil moisture dynamics closely align with those observed in nearby regions, as captured in model outputs or remote sensing data. This metric is critical for evaluating a model's ability to accurately reflect local soil moisture dynamics around each station, thereby supporting robust model validation. To understand spatial patterns of soil moisture dynamics in the study area, an insightful approach based on the spatial representativeness is used (Nicolai-Shaw et al., 2015; Orlowsky & Seneviratne, 2014; Molero et al., 2018). This approach quantifies the area surrounding a SM station of interest for which its temporal dynamics are representative, i.e., its spatial footprint. 350 This area is determined by first calculating Spearman's rank-based correlation coefficient between the time-series of the station under investigation and the surrounding pixels of the studied models and then iteratively removing the furthest pixels away from the station of interest, focusing on keeping 353 only those pixels that have a correlation above a predefined threshold (denoted as rcut). The spa-354 tial representativeness is ultimately defined by the area covered by the convex hull surrounding these stations that exhibit a correlation above rcut threshold (Molero et al., 2018). A convex hull is the smallest polygon that can enclose all the stations that meet the correlation criteria.

358 3.3 Pre-processing and performance validation approach of SM products

The soil moisture products used in this study vary in spatial and temporal resolution, layer depths, and units. Consequently, these datasets undergo preprocessing to standardize their specifications for effective comparison through the following steps:

362 3.3.1 Scaling

365

366

367

368

369

To ensure consistency across the different soil moisture products used in this study, a few scaling procedures are applied:

• The soil moisture products have varying spatial resolutions, such as 0.5° for WaterGAP and GLWS2.0, 0.25° for ESA CCI, and 0.2° for CLM5.0. To enable consistent analysis, the outputs from CLM5.0 and ESA CCI are aggregated to match the 0.5° spatial resolution of WaterGAP and GLWS2.0. In addition to this spatial scaling, all datasets are also aggregated to a monthly temporal resolution to align with the standard resolution of GLWS2.0.





- Furthermore, soil moisture is known to exhibit significant spatial variability. This presents challenges in using single station measurements to accurately represent model simulations across an entire soil moisture (SM) grid, which is set to 0.5° in this study. Direct comparisons between grid-based simulations and point-based observations can introduce substantial errors (Bi et al., 2016). To mitigate this, the study utilizes multiple in situ measurements at each site, which are grouped within the 0.5°x0.5° model pixel resolution area, covering three sites (Benin, Niger, and Senegal). The average of all SM measurements within each site is computed to provide the best possible approximation of the soil moisture at ground level. This approach, adopted by many authors such as Louvet et al. (2015), Bi et al. (2016), and Zhang et al. (2024), ensures a more reliable comparison. To further refine the process, model values are interpolated to the corresponding in situ points using the nearest neighbor method.
- Another challenge in the validation process is the mismatch in depths between the model-based soil moisture (SM) estimates and the SM observations. The ESA CCI captures only near-surface soil moisture, whereas CLM5.0 and in situ data provide soil moisture measurements at various depths, including those within the root zone. In contrast, WaterGAP and GLWS2.0 represent the water content within a single soil moisture reservoir spanning the entire root zone. Consequently, these products are not directly comparable in terms of magnitude (Koster et al., 2009). This issue is addressed in the first subsection.

88 3.3.2 Normalization

The soil water simulated by the GLWS2.0 and WaterGAP models, expressed as water depth (in millimeters), cannot be directly compared to in-situ measurements, ESA CCI data, or CLM5.0 outputs,
which are reported in volumetric fraction. For validation purposes, numerous previous studies have
used a range of normalization techniques to address the inconsistencies among SM estimates derived
from global hydrological models, satellite-based retrievals, and in situ observations (Jung et al., 2019;
Tian et al., 2019). Common methods include percentile-based normalization, moving-window anomalies, and statistical rescaling to standardize datasets, improving alignment across diverse sources and
enhancing the accuracy of validation analyses. In this study, we employed a percentile-based normalization method using the 2nd and 98th percentiles (Eq. 4).

$$w_t = \frac{\theta_t - \theta_{wt}}{\theta_{fc} - \theta_{wt}} \tag{4}$$





In this approach, each data point in the time series θ_t is normalized by subtracting the 2nd percentile of the entire time series from individual monthly values θ_{wt} , followed by dividing the resulting series by the difference between the 98th θ_{fc} and 2nd percentiles of the original time serie θ_{wt} . This method, referred to as "relative wetness" by Tian et al. (2019) and applied in previous studies (e.g., Tian et al. (2019) and references therein), is robust and less sensitive to outliers, making it particularly suitable for our analysis. By normalizing in this way, the approach eliminates information about the original scale, enabling comparisons to focus exclusively on the relative seasonal patterns within each dataset. This avoids biases introduced by absolute magnitudes or imposed statistical alignments, as seen in methods like Raoult et al. (2018), ensuring meaningful comparisons across datasets.

408 3.3.3 Performance validation approach for SM products

After converting soil moisture simulated in the model and derived from satellites into relative wetness, quantitative evaluations were performed on the refined datasets. The seasonality of different SSM time 410 series is analyzed by applying a 12-month rolling boxcar filter. This approach smooths out short-term 411 fluctuations, effectively isolating long-term variations with periods longer than one year. Subtracting 412 this smoothed, long-term component from the original time series reveals the residual signal, which captures the episodic and seasonal variations occurring on timescales shorter than one year. For the 414 validation of surface soil moisture (SSM) and the ESA CCI grid, only soil moisture probes located at 415 depths ≤ 5 cm were considered to ensure consistency. It was assumed that the microwave retrievals 416 from ESA CCI represent moisture content within the top 0-5 cm of the soil column. Three performance metrics were applied in this study: the Pearson correlation coefficient (R), bias, and root-mean-square error (RMSE) for validating with the in situ data, as well as R and RMSE for grid-based validation 419 using the ESA CCI soil moisture data. R is a key statistical metric in this study, as it assesses how well the temporal variability of in situ and soil moisture product time series align. It remains unaffected 421 by differences in mean or variance, which can arise from varying soil properties or scale discrepancies between in situ data and model or satellite footprints (Koster et al., 2009; Gruber et al., 2020; Beck 423 et al., 2021).

25 4 Results and Discussion

4.1 Performance validation of SSM products

In this study, we employed two validation approaches. First, we validated surface soil moisture (SSM) products specifically, ESA CCI, GLWS2.0, WaterGAP, and CLM5.0 by comparing model-soil moisture

https://doi.org/10.5194/egusphere-2025-4600 Preprint. Discussion started: 14 October 2025 © Author(s) 2025. CC BY 4.0 License.





- with in situ measurements taken at a depth of 5 cm across different study sites in Benin, Niger, and
- 430 Senegal. Our analysis emphasized the temporal correspondence between the datasets (e.g., time/phase
- 431 lags, dry and wet spell event periods) rather than the magnitudes. Additionally, deseasonalized
- 432 and episodic time series were compared with the corresponding in situ time series to further assess
- 433 consistency and alignment. Second, we compared the GLWS2.0, WaterGAP, and CLM5 models against
- 434 the ESA CCI gridded soil moisture data.

4.1.1 In situ-based data validation of different SSM products

- 436 The normalized soil moisture time series from ESA CCI, GLWS2.0, WaterGAP, and CLM5.0, along
- with the in situ time series at each study site are overlaid and presented in Figure 3.





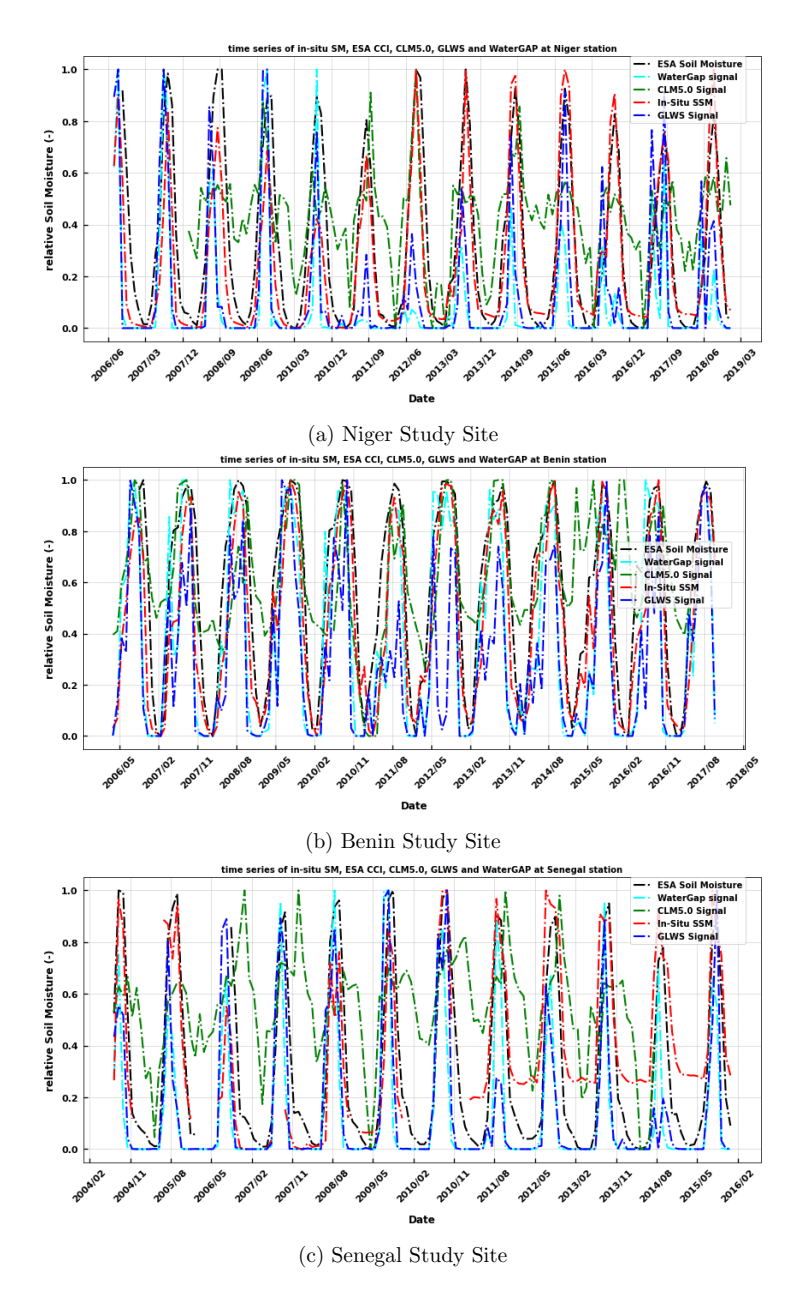


Figure 3: Normalized soil moisture time series for in situ measurements, ESA CCI, GLWS2.0, Water-GAP, and CLM5.0 at three distinct study sites at a depth of $5~\mathrm{cm}$.

The ESA CCI, GLWS2.0 and CLM5.0 SM products effectively replicate the seasonal dynamics of monthly surface soil moisture (SSM) observed in ground-based measurements across different sites, demonstrating their robustness in capturing the effects of varying land cover and climate conditions in the region. The seasonal changes in soil moisture at a depth of 5 cm show marked variability, likely https://doi.org/10.5194/egusphere-2025-4600 Preprint. Discussion started: 14 October 2025 © Author(s) 2025. CC BY 4.0 License.





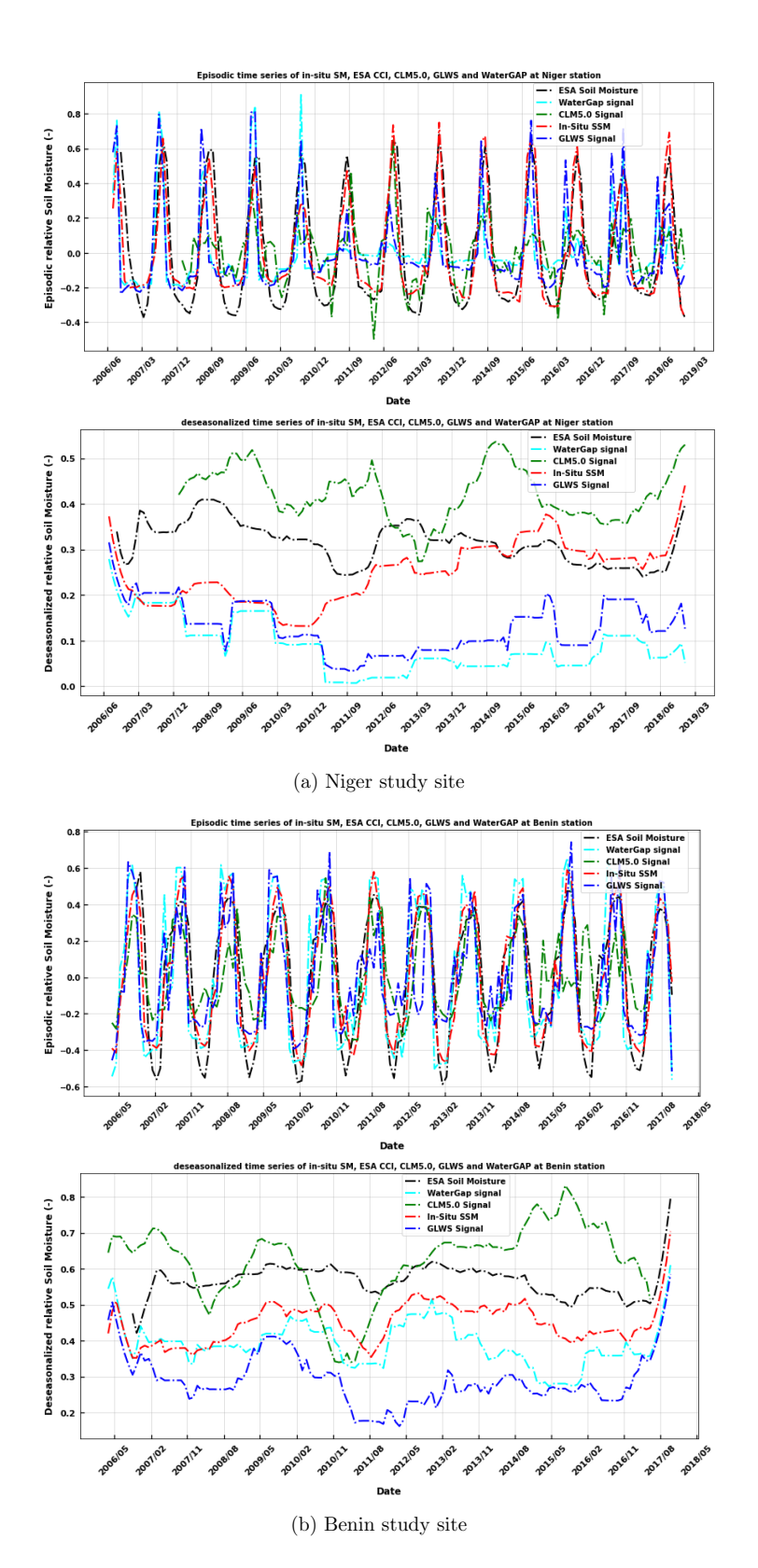
driven by the influence of the monsoon across the West African region. Similar dynamics are observed over the Tibetan Plateau, where soil moisture cycles are shaped significantly by the South Asian summer monsoon (Bi et al., 2016). These patterns underscore the importance of regional monsoon systems in determining soil moisture fluctuations across distinct climatic zones. In situ observations 445 in Niger and Senegal reveal a typical Sahelian seasonal cycle, marked by a distinct wet season from June to October, while the Benin site, located in the Sudanian climate zone, experiences a rainy 447 season extending from April to October, along with a longer monsoon period. The statistics from the normalized SSM signals, as presented in Table 2, highlight the performance of various datasets in terms of synchronization and correlation with in-situ measurements. In Benin, ESA, GLWS2.0, and 450 WaterGap generally exhibit strong synchronization, with time lags close to 0 months. These datasets 451 also demonstrate high correlations (ESA: 0.894, WaterGap: 0.856, GLWS2.0: 0.752). In Senegal, these same datasets show minimal time lag (ranging from 0 to 1 month), though the correlations 453 are somewhat weaker (ESA: 0.646, WaterGap: 0.637, GLWS2.0: 0.574). In Niger, ESA remains well-aligned with in-situ measurements (0-month lag and a 0.864 correlation), while both GLWS2.0 455 and WaterGap experience slight delays (1-month lag), accompanied by weaker correlations (0.655 and 0.515, respectively).

458 4.1.2 SSM seasonality

To better highlight events in the time series, a deseasonalization method is applied. The seasonal maps derived from this process are presented in Fig. 4.











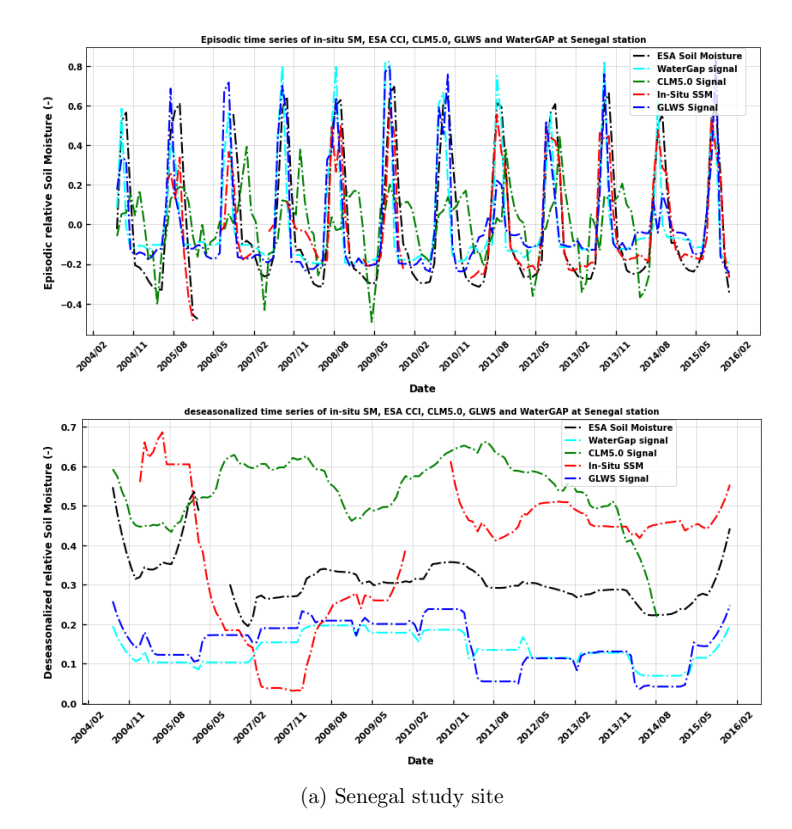


Figure 4: Episodic and Deseasonalized time series for soil moisture across study sites.

The analysis of episodic and deseasonalized time series for soil moisture across Senegal, Niger, 461 and Benin reveals distinct regional patterns influenced by the West African Monsoon (WAM). In the Sahelian zones of Niger and Senegal, typical seasonal cycles show sharp increases in soil moisture during the monsoon (June to October) and declines in the dry season (November to May). Deseasonalized 464 data highlight anomalies, such as unseasonal rainfall or dry spells, which suggest shifts in the timing 465 or intensity of the monsoon and potential impacts of climate variability, such as droughts or flooding. 466 In Benin, located in the Sudanian climate zone, a longer rainy season (April to October) leads to a more extended period of increased soil moisture, with anomalous events like flooding or unexpected dry spells reflecting changes in rainfall distribution. Overall, deseasonalizing the time series reveals 469 how soil moisture is sensitive to shifts in the monsoon, with delayed rains in the Sahel potentially causing droughts, while early or heavy rains in Benin could lead to flooding or soil saturation. The correlation between the seasonality of the ESA CCI product and the in situ data is generally high, 472 exceeding 0.9 for episodic time series across all sites. At the Benin site, ESA CCI demonstrates the 473 strongest performance, followed by the assimilation-based model GLWS2.0. Meanwhile, at the Niger and Senegal sites, WaterGAP also performs well, ranking closely behind ESA CCI.





Table 2: Statistics from the normalized SSM time series.

	Benin				Niger				Senegal			
	Lag (month	ı) corr	bias	rmse	Lag (month)	corr	bias	rmse	Lag (month)	corr	bias	rmse
Insitu - ESA	0	0.894	-0.120	0.178	0	0.864	-0.073	0.164	0	0.646	0.046	0.214
Insitu - GLWS2.0	0	0.752	0.161	0.284	1	0.655	0.12	0.276	0	0.574	0.222	0.356
Insitu – WaterGap	0	0.856	0.060	0.211	1	0.515	0.161	0.312	1	0.637	0.241	0.351
Insitu - CLM5	6	0.618	-0.168	0.548	-18	0.497	-0.183	0.464	17	0.437	-0.112	0.470

Table 3: Statistics from the normalized SSM time series.

	Benin			Niger			Senegal				
	corr	bias	rmse	corr	bias	rmse	corr	bias	rmse		
	Episodic time series										
Insitu – ESA	0.932	-0.003	0.128	0.926	-0.006	0.123	0.900	-0.033	0.158		
Insitu - GLWS2.0	0.762	0.002	0.225	0.617	0.000	0.234	0.661	-0.014	0.215		
Insitu – WaterGap	0.861	0.002	0.200	0.509	0.000	0.251	0.702	-0.008	0.201		
Insitu – CLM5	0.710	-0.006	0.240	0.505	-0.002	0.224	0.345	-0.017	0.256		
	Deseasonalized time series										
Insitu - ESA	0.765	-0.117	0.123	-0.182	-0.067	0.108	0.340	0.082	0.178		
Insitu - GLWS2.0	0.400	0.158	0.174	0.043	0.119	0.145	-0.470	0.236	0.309		
Insitu – WaterGap	0.588	0.058	0.079	-0.287	0.161	0.188	-0.412	0.246	0.308		
Insitu – CLM5	0.096	-0.175	0.208	0.046	-0.168	0.188	-0.350	-0.172	0.280		

4.1.3 ESA CCI grid based evaluation of the different models

terGAP, and CLM5.0) a grid-based comparison was conducted using remotely sensed surface soil
moisture (SSM) data from ESA CCI. Figure 4 displays the Pearson correlation coefficient (R) and
root-mean-square error (RMSE) metrics, providing insights into how well the GLWS2.0, WaterGAP,
and CLM5.0 models perform relative to the ESA CCI grid. In this figure, gaps in the data particularly noticeable in forested and densely vegetated areas (shown as white regions near the coastline)
highlight areas where soil moisture estimates are challenging. This data masking in the ESA CCI
SSM datasets occurs because microwave-based observations typically exclude areas with moderate to
dense vegetation due to the strong attenuation of soil signals by the vegetation canopy (Dorigo et al.,
2017).

The figure also reveals that the patterns in RMSE and correlation metrics vary with land cover type, demonstrating that land cover exerts a clear influence on the performance of these models.

GLWS2.0 shows a notably lower RMSE than the other models across the region and exhibits strong



492



- spatial consistency across various land cover types. The lowest RMSE values for GLWS2.0 are observed
- in the semi-arid Sahel regions, likely due to its effective assimilation process that better captures soil moisture dynamics in these environments.

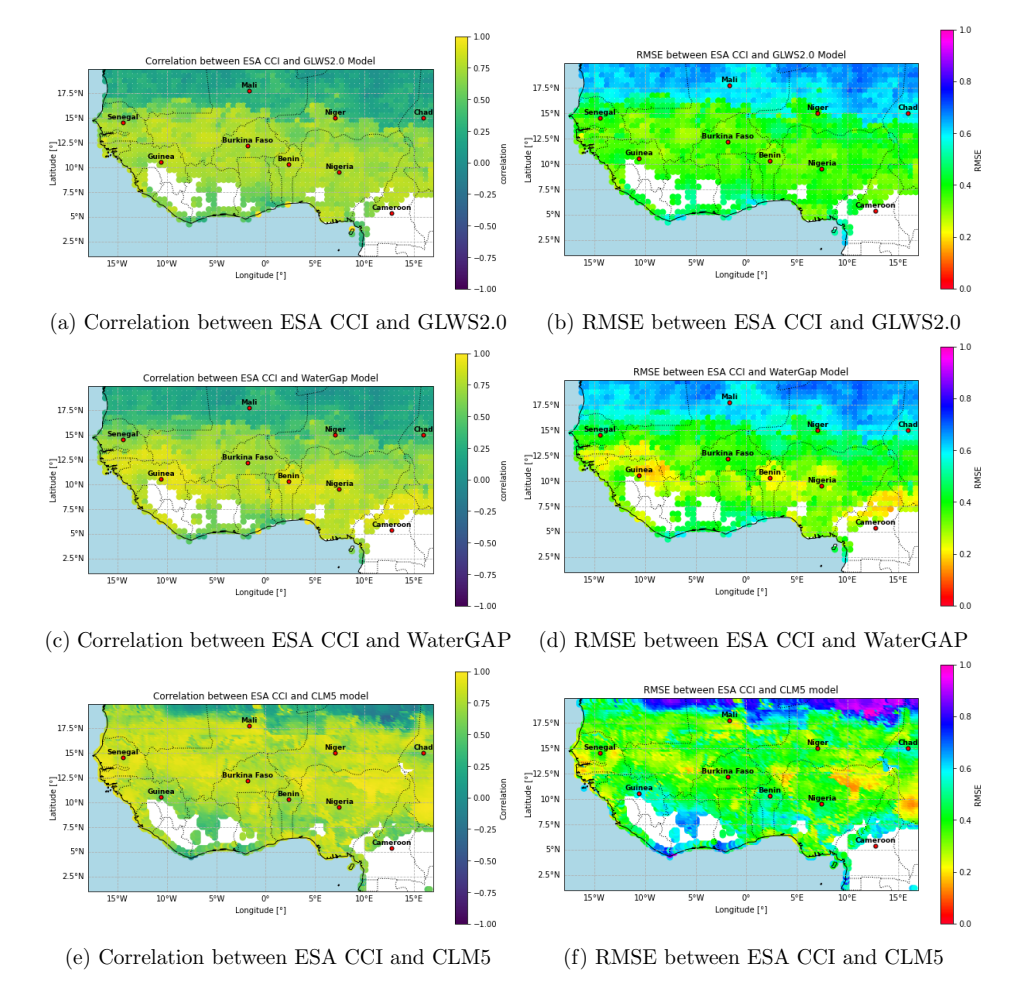


Figure 5: Pearson correlation coefficient (R) and RMSE metrics illustrating the performance of GLWS2.0, WaterGAP, and CLM5 models relative to the ESA CCI grid.

The figure underscores the complexities of soil moisture modeling across the diverse climates and land covers of the West African region, where model performance and error metrics vary significantly.

While GLWS2.0 demonstrates spatial consistency across different land-cover types with relatively low RMSE values, this consistency is not as evident in other models. RMSE values are generally lower in the northern part of West Africa but higher in the southern regions. This variation may be attributed to the sporadic nature of soil moisture in these areas, where conditions are highly dependent on occasional rainfall events. In these regions, soil moisture levels can shift rapidly, with dry conditions prevailing and only brief, intense increases in moisture following rainfall. Both the satellite data





(ESA CCI) and the hydrological models encounter challenges in accurately capturing these short-lived, extreme moisture events. However, because arid and semi-arid regions experience prolonged dry spells, the overall RMSE between model predictions and satellite observations remains relatively low, despite the missed short-term fluctuations. This pattern underscores the inherent challenges of modeling soil 504 moisture in arid and semi-arid regions, where infrequent but intense moisture changes add complexity 505 to the dynamics. Additionally, the figures show that GLWS2.0 demonstrates stronger correlation with 506 ESA CCI data compared to other models, particularly WaterGAP, which does not show dependency on land-cover types. This correlation is generally higher in southern West Africa and weaker in the 508 north, where low soil moisture values make it difficult to discern clear patterns. In the southern regions, 509 more frequent and consistent rainfall leads to stable soil moisture levels, allowing moisture dynamics 510 to be easier to predict. Consequently, the spatial correlation pattern between GLWS2.0 and ESA CCI soil moisture data reveals a clear latitudinal gradient aligned with annual rainfall and climate zones. 512 This pattern is particularly evident in semi-arid regions that serve as transition zones between wet and 513 dry climates, where the highest correlation values are observed (i.e. area between 9.5°N and 15°N). 514 Such transitional regions, including the Indian subcontinent, the North American Great Plains, and southeastern Brazil, also exhibit increased correlation values due to pronounced seasonal and interannual variability in soil moisture (SM) measurements (Al-Yaari et al., 2014). Similar findings were 517 reported by Jung et al. (2019) over West Africa, where an evaluation of spatial correlations between 518 GRACE-based assimilation, SSM simulations and satellite-derived SSM products (ASCAT, SMOS, 519 and SMAP) indicated strong correlation patterns in transitional zones. This consistency suggests that SM measurements in these regions are particularly sensitive to seasonal dynamics and the distinct 521 cycles of wet and dry phases. Moreover, GLWS2.0 effectively captures the general pattern of soil moisture in the south, where soils retain moisture better and vegetation moderates fluctuations.

524 4.2 Spatial Representativeness

Figure 5 illustrates the Spatial Representativeness (SR) of ESA CCI, GLWS2.0, WaterGAP, and CLM5.0 using a cutoff Spearman correlation of 0.6, which effectively highlights how well each soil moisture product reflects observed soil moisture dynamics at each study site. This similarity threshold distinguishes between datasets that demonstrate moderate to strong agreement with in situ observations, categorizing them as performing well (correlation > 0.6) or less effectively (correlation ≤ 0.6) in capturing real-world variations. Notably, only ESA CCI and GLWS2.0 exhibit Spearman correlations greater than 0.6 with in situ data, indicating that these models accurately capture the spatial and temporal dynamics of soil moisture within their respective spatial footprints. This alignment suggests

https://doi.org/10.5194/egusphere-2025-4600 Preprint. Discussion started: 14 October 2025 © Author(s) 2025. CC BY 4.0 License.





that their soil moisture estimates correlate quite well with the observed time series. Furthermore, the efficacy of the GLWS2.0 assimilation process likely enhances its ability to reflect real-world soil 534 moisture conditions, particularly in arid and semi-arid regions characterized by sporadic moisture changes. In contrast, the lower correlations observed for WaterGAP and CLM5.0 point to limitations 536 in these models' capacity to represent soil moisture variability at finer spatial scales. Overall, these 537 findings underscore the importance of integrating observational data to enhance model accuracy in 538 representing high-resolution soil moisture dynamics, suggesting that ESA CCI and GLWS2.0 are better suited for regional applications requiring high spatial sensitivity. Although the SR approach has not previously been applied to the satellite/model SM products examined in this study, it has proven 541 effective for validating other SM products across various regions worldwide. For example, in the Little 542 Washita watershed in the United States and the Yanco area in Australia, spatial representativeness has been used to explore the connections between SM spatial scales and timescales within the 50 km satellite footprint of SMOS, AMSR2, and ECMWF SM products (Molero et al., 2018). These 545 authors demonstrate that the spatial representativeness of surface soil moisture increases with longer 546 timescales, but with greater variability in these regions. Nicolai-Shaw et al. (2015) showcased the robustness and effectiveness of this approach for selecting appropriate soil moisture products. By applying it to analyze the temporal dynamics of absolute soil moisture across North America, they 549 compared in situ observations with the European Space Agency's ECV-SM and ERA-Land datasets. 550 Orlowsky & Seneviratne (2014) demonstrating the robustness of this parameter-free method in cli-551 matology to quantify the spatial footprint of weather stations across Europe. Their findings show that temperature data generally exhibit greater representativeness than precipitation, with significant 553 seasonal changes influenced by atmospheric circulation patterns, particularly in boreal winter.





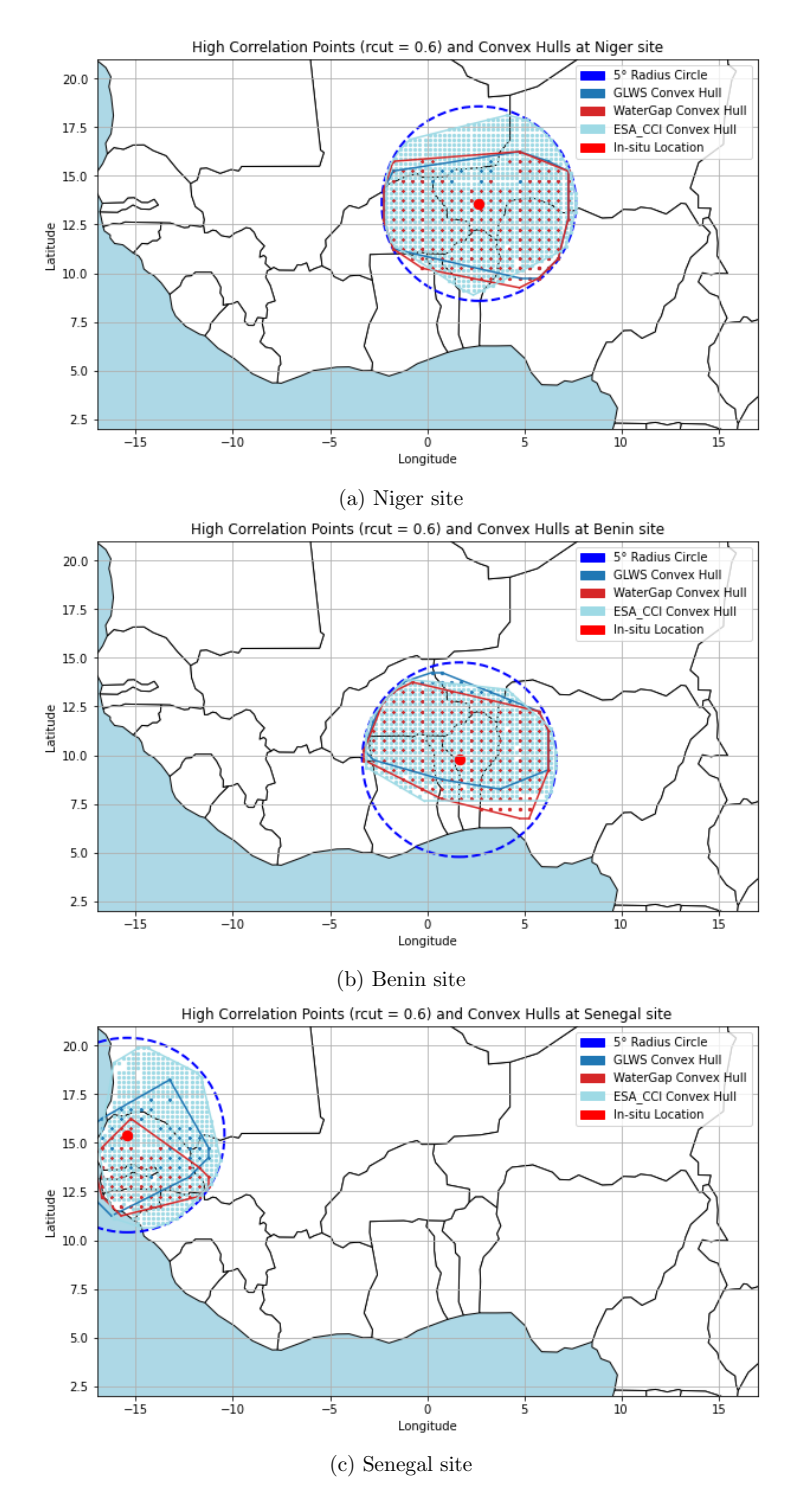


Figure 6: Spatial footprint of soil moisture products represented by a blue circle with a radius of 5° around each site, indicated in red. The convex hulls in light and dark blue represent the areas for which ESA CCI and GLWS2.0 exceed the specified cutoff threshold of 0.6, respectively.



560

581



Retrieving the root-zone soil moisture from GLWS2.0 and WaterGap and validating its dynamics using in-situ and CLM5

An analytical solution to Richards' equation is used to convert water content from GLWS2.0 and WaterGAP to different depths, enabling comparison of model-derived root zone soil moisture with in-situ observations across depths (Figures 6 to 9).

• Projection depth (node depth) = 5 cm

GLWS2.0, which incorporates GRACE/FO data, demonstrates superior performance than Wa-561 terGAP and yields results comparable to those of CLM5.0 in capturing the monthly root zone soil 562 moisture (RZSM) dynamics at the Niger and Benin sites at this depth (Figure 6). However, the 563 temporal dynamics at the Senegal site are less consistent, particularly during the initial two years (2004–2006) of the in situ observation system. This discrepancy can be partially attributed to the Senegal site being represented by a single station, unlike Niger and Benin, which have at least three 566 stations at different locations. The limited data from a single station poses challenges in accurately 567 representing model simulations over a broader 0.5° soil moisture grid study (Louvet et al., 2015). Fur-568 thermore, the WaterGAP model struggles to capture long-term (2006–2018) seasonal dynamics at all sites as recorded by in situ sensors. At a depth of 5 cm, a comparison of model performances in capturing seasonal soil moisture dynamics shows that the ESA CCI model aligns most closely with in situ 571 measurements. ESA CCI achieves the lowest RMSE and the highest R^2 values across all study sites: Benin (RMSE = 0.194, $R^2 = 0.714$), Niger (RMSE = 0.166, $R^2 = 0.663$), and Senegal (RMSE = 0.213, $R^2 = 0.533$). The GLWS2.0 assimilation-based model ranks second in accuracy, with corresponding 574 values in Benin (RMSE = 0.336, R^2 = 0.224), Niger (RMSE = 0.317, R^2 = -0.031), and Senegal (RMSE = 0.307, R^2 = 0.403). CLM5.0 provides performance metrics similar to those of GLWS2.0, 576 with values in Benin (RMSE = 0.339, $R^2 = 0.229$), Niger (RMSE = 0.339, $R^2 = -0.351$), and Senegal $(RMSE = 0.386, R^2 = 0.257)$. These results indicate that ESA CCI demonstrates the highest accuracy in reflecting seasonal soil moisture patterns, while GLWS2.0 and CLM5.0 show comparable but lower precision in fitting observed in situ measurements across all sites. 580

• Projection depth (node depth) = 10 cm, 40 cm, 100 cm

As illustrated in figures 7, 8, and 9, which represent RZSM at depths of 10, 40, and 100 cm respectively, both GLWS2.0 and CLM5.0 capture reasonably the seasonal dynamics of soil moisture at the Niger and Benin sites. These models show good alignment with in situ measurements across different depths, demonstrating their ability to reflect seasonal moisture changes as recorded by the local





sensors. However, the WaterGAP model does not reflect this seasonality effectively. At the Senegal site, these seasonal patterns are notably absent, likely due to previously mentioned issues with the limited data from a single station, which may not fully represent local soil moisture variability at the model's grid scale (0.5° resolution). Furthermore, seasonal consistency in GLWS2.0 projections across 589 depths is less reliable at the Senegal site, situated near the coastline. This discrepancy could stem 590 from coastal regions' unique characteristics, such as tidal influences and potential signal interference 591 from the nearby ocean, which may impact the accuracy of GRACE/-FO-based observations used in the model's assimilation process. In comparing RZSM estimates retrieved from GLWS2.0 and 593 WaterGAP to in situ observations and the physically based model CLM5.0 at depths of 10 cm and 40 594 cm, CLM5.0 demonstrates slightly better performance. This is reflected in CLM5.0's smaller RMSE 595 and higher R² values across the study sites, indicating a closer alignment with observed moisture dynamics. However, at a depth of 100 cm, GLWS2.0 performs marginally better than CLM5.0, with 597 slightly lower RMSE and higher R² metrics, suggesting a potential advantage of GLWS2.0 in capturing 598 RZSM dynamics at this depth. Overall, while GLWS2.0 exhibits solid performance, particularly in 599 comparison to WaterGAP, WaterGAP's RZSM estimates show more significant discrepancies from both in situ measurements and the results provided by CLM5.0, especially at all depths observed. In addition, CLM5.0 performed quite poor at 5cm, but relatively good at greater depths. This might 602 be related to inclusion of measurement data by ESA CCI at 5cm., while CLM5.0 did not have data 603 assimilation at this depth. The influence of 5 cm soil moisture measurements diminishes at greater 604 depths, while apparently the model for vertical soil moisture transport scheme that CLM5.0 uses is better than for the other models. GLWS2.0, on the other hand, benefits from GRACE-based data assimilation at depth, which likely explains its comparatively stronger performance at 100 cm.

5 Conclusions and implications

This study assessed root-zone soil moisture (RZSM) dynamics across West Africa between 2003 and 2019 using multiple data products, including GLWS2.0, WaterGAP, CLM5.0, ESA CCI v0.81 product, and in-situ measurements. Results show that ESA CCI, CLM5.0 and GLWS2.0 effectively capture the seasonal soil moisture dynamics, while WaterGAP performs less reliably. ESA CCI demonstrates the strongest temporal alignment with in-situ observations, characterized by near-zero time lags and high correlation across all regions. CLM5.0 and GLWS2.0 show moderate to good performance, with ESA CCI remaining the most reliable overall in terms of both synchronization and correlation.

A grid-based validation of GLWS2.0, WaterGAP, and CLM5.0 models against ESA CCI data which
has shown high accuracy in the region reveals that CLM5.0 and GLWS2.0 correlate more strongly with

https://doi.org/10.5194/egusphere-2025-4600 Preprint. Discussion started: 14 October 2025 © Author(s) 2025. CC BY 4.0 License.





ESA CCI across West Africa, displaying a distinct latitudinal gradient aligned with annual rainfall and climate zones. This gradient, particularly strong in the transition zones between wet and dry climates (9.5°N to 15°N) as similarly noted by Jung et al. (2019), highlights their capacity to capture spatial patterns in SM dynamics. In contrast, WaterGAP lacks this dependency on land-cover types, suggesting its limitations in capturing regional SM variations.

To evaluate how well each product captures spatially coherent soil moisture (SM) dynamics, a 623 Spearman correlation threshold of 0.6 was applied. This helped identify the extent to which temporal SM variations at a given location resemble those in surrounding areas. The results show that ESA 625 CCI, GLWS2.0, and WaterGAP consistently meet this threshold around the studied sites, indicating 626 that these models accurately capture the spatial and temporal dynamics of SM within their respective 627 spatial footprints. Although this approach has not previously been applied to the satellite/model SM products examined in this study, it has proven effective for validating other SM products across various 629 regions worldwide (Orlowsky & Seneviratne, 2014; Nicolai-Shaw et al., 2015; Molero et al., 2018). 630 However, it is important to acknowledge several limitations that may affect both the in-situ and grid-631 based validation, as well as the spatial footprint analysis. First, the limited number of in-situ probes at each study site may not adequately capture the local variability in soil moisture (SM), especially when compared to the coarser 0.5° spatial resolution of the models. Additionally, the availability of ESA 634 CCI data is often restricted in forested and densely vegetated regions due to the strong attenuation 635 of microwave signals by vegetation canopies, as noted by Dorigo et al. (2017). Another source of 636 uncertainty lies in the mismatch between the spatial representativeness of point-based observations and the model grid size, which can introduce discrepancies in the validation process. Moreover, the 638 normalization applied to the datasets, while useful for comparative purposes, may have masked true 639 differences in SM magnitudes across products. Finally, temporal gaps in data coverage—whether in in-situ records or satellite-derived products—can affect the consistency and reliability of the validation outcomes. 642

An analytical solution of Richards' equation was applied to translate water content from the single soil moisture reservoir from WaterGAP and GLWS2.0 to various depths. At 5 cm soil depth, ESA CCI consistently shows the closest alignment with in situ SM data, achieving the lowest RMSE and the highest R^2 values across all study sites. The GLWS2.0 and CLM5.0 models rank next in accuracy, with GLWS2.0 showing RMSE values around 0.317–0.336 and R^2 values from -0.031 to 0.403, while CLM5.0 demonstrates similar metrics, indicating that both provide comparable but less precise tracking of observed soil moisture dynamics. The findings reinforce prior in situ and grid-based validation results and spatial footprint analysis, which highlight GLWS2.0's sensitivity to the top 0–5





cm soil layer. At greater depths (10, 40, and 100 cm), the GLWS2.0 model reasonably captures the seasonal SM dynamics observed in both in situ measurements and CLM5.0 outputs at the Benin and Niger sites. However, these seasonal patterns are notably absent at the Senegal site, likely due to the limited number of probes and signal contamination from the nearby ocean.

Overall, GLWS2.0 performs better than WaterGAP at various depths, largely due to the advantages provided by the GRACE/-FO data assimilation process, which enhances its accuracy in capturing root zone soil moisture dynamics. Additionally, even without GRACE/-FO data assimilation, CLM5.0 shows substantially better performance than WaterGAP across all study sites, reflecting its stronger capability to track soil moisture variations in West Africa.

The novel application of this depth-translation approach, based on analytical solutions of Richards' 660 equation, enabled the projection of water content from a single soil moisture reservoir to various depths across West Africa, providing insights that go beyond traditional SM analysis in the region. This 662 methodology not only extends the shallow vertical range typically captured by microwave satellite 663 sensors, but it also offers a way to differentiate surface and groundwater storage variations within the 664 GRACE/-FO data, potentially expanding our understanding of water storage dynamics in complex hydrological settings. By enhancing the representation of SM across different depths, this framework can improve agricultural forecasting and deepen our understanding of water cycle interactions across 667 diverse landscapes, especially in regions where accurate SM data are essential for sustainable water 668 management.

670 Competing interests

Harrie-Jan Hendricks Franssen is a member of the editorial board of Hydrology and Earth System
 Sciences. The authors declare that they have no other competing interests.

Author contributions

LY: Data curation, methodology, software, formal analysis, visualization, interpretation, validation, writing (original draft, review and editing). JK: Conceptualization, methodology, writing (review and editing), supervision. BO: Methodology, model running, writing (review and editing). HG:
Interpretation, writing (review and editing). HJHF: Conceptualization, supervision, writing (review and editing).





679 Acknowledgments

- 680 We acknowledge funding through University of Bonn's SDG fellowship program, and from Deutsche
- 681 Forschungsgemeinschaft (DFG, German Research Foundation), SFB 1502/1-2022 (Projektnummer:
- 682 450058266).

References

- 684 Al-Yaari, A., Wigneron, J. P., Ducharne, A., Kerr, Y., de Rosnay, P., de Jeu, R., Govind, A., Al Bitar,
- A., Albergel, C., Muñoz-Sabater, J., Richaume, P., & Mialon, A. (2014). Global-scale evaluation of
- two satellite-based passive microwave soil moisture datasets (SMOS and AMSR-E) with respect to
- Land Data Assimilation System estimates. Remote Sensing of Environment, 149, 181–195. https:
- 688 //doi.org/10.1016/j.rse.2014.04.006
- 689 Bartalis, Z., Wagner, W., Naeimi, V., Hasenauer, S., Scipal, K., Bonekamp, H., Figa, J., & Ander-
- son, C. (2007). Initial soil moisture retrievals from the METOP-A Advanced Scatterometer (AS-
- 691 CAT). Geophysical Research Letters, 34(20). https://doi.org/10.1029/2007GL031088. _eprint:
- https://onlinelibrary.wiley.com/doi/pdf/10.1029/2007GL031088
- Baup, F., Mougin, E., de Rosnay, P., Hiernaux, P., Frappart, F., Frison, P. L., Zribi, M., & Viarre, J.
- 694 (2011). Mapping surface soil moisture over the Gourma mesoscale site (Mali) by using ENVISAT
- ASAR data. Hydrology and Earth System Sciences, 15(2), 603-616. https://doi.org/10.5194/
- hess-15-603-2011. Publisher: Copernicus GmbH
- 697 Bayat, B., Oloruntoba, B., Montzka, C., Vereecken, H., & Hendricks Franssen, H.-J. (2023). Im-
- plications for sustainable water consumption in Africa by simulating five decades (1965–2014) of
- groundwater recharge. Journal of Hydrology, 626, 130288. https://doi.org/10.1016/j.jhydrol.
- 700 2023.130288
- 701 Beck, H. E., Pan, M., Miralles, D. G., Reichle, R. H., Dorigo, W. A., Hahn, S., Sheffield, J.,
- Karthikeyan, L., Balsamo, G., Parinussa, R. M., van Dijk, A. I. J. M., Du, J., Kimball, J. S.,
- Vergopolan, N., & Wood, E. F. (2021). Evaluation of 18 satellite- and model-based soil moisture
- products using in situ measurements from 826 sensors. Hydrology and Earth System Sciences, 25(1),
- 705 17-40. https://doi.org/10.5194/hess-25-17-2021. Publisher: Copernicus GmbH
- 706 Bi, H., Ma, J., Zheng, W., & Zeng, J. (2016). Comparison of soil moisture in GLDAS model
- vor simulations and in situ observations over the Tibetan Plateau. Journal of Geophysical Re-





- search: Atmospheres, 121(6), 2658-2678. https://doi.org/10.1002/2015JD024131. _eprint:
- https://onlinelibrary.wiley.com/doi/pdf/10.1002/2015JD024131
- 710 Brocca, L., Ciabatta, L., Massari, C., Camici, S., & Tarpanelli, A. (2017). Soil Moisture for Hy-
- drological Applications: Open Questions and New Opportunities. Water, 9(2), 140. https:
- //doi.org/10.3390/w9020140. Number: 2 Publisher: Multidisciplinary Digital Publishing In-
- 713 stitute
- 714 Cappelaere, B., Descroix, L., Lebel, T., Boulain, N., Ramier, D., Laurent, J. P., Favreau, G.,
- Boubkraoui, S., Boucher, M., Bouzou Moussa, I., Chaffard, V., Hiernaux, P., Issoufou, H. B. A.,
- Le Breton, E., Mamadou, I., Nazoumou, Y., Oi, M., Ottlé, C., & Quantin, G. (2009). The AMMA-
- CATCH experiment in the cultivated Sahelian area of south-west Niger Investigating water cycle
- response to a fluctuating climate and changing environment. Journal of Hydrology, 375(1), 34–51.
- 719 https://doi.org/10.1016/j.jhydrol.2009.06.021
- 720 Chartzoulakis, K. & Bertaki, M. (2015). Sustainable Water Management in Agriculture under Climate
- Change. Agriculture and Agricultural Science Procedia, 4, 88-98. https://doi.org/10.1016/j.
- 722 aaspro.2015.03.011
- 723 Chen, F., Crow, W. T., Bindlish, R., Colliander, A., Burgin, M. S., Asanuma, J., & Aida, K. (2018).
- Global-scale evaluation of SMAP, SMOS and ASCAT soil moisture products using triple collocation.
- Remote Sensing of Environment, 214, 1-13. https://doi.org/10.1016/j.rse.2018.05.008
- 726 Chisanga, C. B., Phiri, D., & Mubanga, K. H. (2024). Multi-decade land cover/land use dynamics
- and future predictions for Zambia: 2000-2030. Discover Environment, 2(1), 38. https://doi.org/
- 728 10.1007/s44274-024-00066-w
- 729 Defourny, P., Lamarche, C., Brockmann, C., Boettcher, M., Bontemps, S., De Maet, T., Duveiller,
- G., Harper, K., Hartley, A., Kirches, G., Moreau, I., Peylin, P., Ottlé, C., J, R., Van Bogaert, E.,
- Ramoino, F., Albergel, C., & Arino, O. (2023). Observed annual global land-use change from 1992
- to 2020 three times more dynamic than reported by inventory-based statistics. https://maps.elie.
- ucl.ac.be/CCI/viewer/download.php. In preparation
- 734 Diatta, S. & Fink, A. H. (2014). Statistical relationship between remote climate indices and West
- African monsoon variability. International Journal of Climatology, 34(12), 3348–3367. https:
- 736 //doi.org/10.1002/joc.3912
- Dorigo, W., Wagner, W., Albergel, C., Albrecht, F., Balsamo, G., Brocca, L., Chung, D., Ertl, M.,
- Forkel, M., Gruber, A., Haas, E., Hamer, P. D., Hirschi, M., Ikonen, J., de Jeu, R., Kidd, R., Lahoz,





- 739 W., Liu, Y. Y., Miralles, D., Mistelbauer, T., Nicolai-Shaw, N., Parinussa, R., Pratola, C., Reimer,
- 740 C., van der Schalie, R., Seneviratne, S. I., Smolander, T., & Lecomte, P. (2017). ESA CCI Soil
- Moisture for improved Earth system understanding: State-of-the art and future directions. Remote
- Sensing of Environment, 203, 185-215. https://doi.org/10.1016/j.rse.2017.07.001
- 743 Dorigo, W., Xaver, A., Vreugdenhil, M., Gruber, A., Hegyiová, A., Sanchis-Dufau, A., Zamo-
- jski, D., Cordes, C., Wagner, W., & Drusch, M. (2013). Global Automated Quality Con-
- $_{745}$ trol of In Situ Soil Moisture Data from the International Soil Moisture Network. Va-
- dose Zone Journal, 12(3), vzj2012.0097. https://doi.org/10.2136/vzj2012.0097. _eprint:
- https://onlinelibrary.wiley.com/doi/pdf/10.2136/vzj2012.0097
- Dorigo, W. A., Wagner, W., Hohensinn, R., Hahn, S., Paulik, C., Xaver, A., Gruber, A., Drusch,
- M., Mecklenburg, S., van Oevelen, P., Robock, A., & Jackson, T. (2011). The International Soil
- Moisture Network: a data hosting facility for global in situ soil moisture measurements. Hydrology
- and Earth System Sciences, 15(5), 1675-1698. https://doi.org/10.5194/hess-15-1675-2011.
- 752 Publisher: Copernicus GmbH
- Entekhabi, D., Njoku, E. G., O'Neill, P. E., Kellogg, K. H., Crow, W. T., Edelstein, W. N., Entin,
- J. K., Goodman, S. D., Jackson, T. J., Johnson, J., Kimball, J., Piepmeier, J. R., Koster, R. D.,
- Martin, N., McDonald, K. C., Moghaddam, M., Moran, S., Reichle, R., Shi, J. C., Spencer, M. W.,
- Thurman, S. W., Tsang, L., & Van Zyl, J. (2010). The Soil Moisture Active Passive (SMAP) Mis-
- sion. Proceedings of the IEEE, 98(5), 704-716. https://doi.org/10.1109/JPROC.2010.2043918.
- Conference Name: Proceedings of the IEEE
- 759 Evensen, G. (2003). The Ensemble Kalman Filter: theoretical formulation and practical implementa-
- tion. Ocean Dynamics, 53(4), 343-367. https://doi.org/10.1007/s10236-003-0036-9
- 761 Famiglietti, J. S. & Wood, E. F. (1994). Multiscale modeling of spatially variable water and energy
- balance processes. Water Resources Research, 30(11), 3061-3078. https://doi.org/10.1029/
- 94WR01498. _eprint: https://onlinelibrary.wiley.com/doi/pdf/10.1029/94WR01498
- ⁷⁶⁴ Faridani, F., Farid, A., Ansari, H., & Manfreda, S. (2017). A modified version of the SMAR model
- for estimating root-zone soil moisture from time-series of surface soil moisture. Water SA, 43(3),
- 766 492-498. https://doi.org/10.4314/wsa.v43i3.14. Number: 3
- Fatras, C., Frappart, F., Mougin, E., Grippa, M., & Hiernaux, P. (2012). Estimating surface soil
- moisture over Sahel using ENVISAT radar altimetry. Remote Sensing of Environment, 123, 496-
- 769 507. https://doi.org/10.1016/j.rse.2012.04.013





- 770 Fink, D., Hochachka, W. M., Zuckerberg, B., Winkler, D. W., Shaby, B., Munson, M. A., Hooker, G.,
- 771 Riedewald, M., Sheldon, D., & Kelling, S. (2010). Spatiotemporal exploratory models for broad-scale
- survey data. Ecological Applications, 20(8), 2131-2147. https://doi.org/10.1890/09-1340.1.
- -eprint: https://onlinelibrary.wiley.com/doi/pdf/10.1890/09-1340.1
- 774 Galle, S., Manuela, G., Peugeot, C., Bouzou-Moussa, I., Cappelaere, B., Demarty, J., Mougin, E.,
- Panthou, G., Adjomayi, P., Agbossou, E., Abdramane, B., Boucher, M., Cohard, J.-M., Descloitres,
- M., Descroix, L., Diawara, M., Do, M., Favreau, G., Fabrice, G., & Wilcox, C. (2018). AMMA-
- 777 CATCH, a Critical Zone Observatory in West Africa Monitoring a Region in Transition. https:
- 778 //doi.org/10.2136/vzj2018.03.0062
- 779 Gavahi, K., Abbaszadeh, P., Moradkhani, H., Zhan, X., & Hain, C. (2020). Multivariate Assimilation
- 780 of Remotely Sensed Soil Moisture and Evapotranspiration for Drought Monitoring. Journal of
- 781 Hydrometeorology, 21(10), 2293-2308. https://doi.org/10.1175/JHM-D-20-0057.1. Publisher:
- American Meteorological Society Section: Journal of Hydrometeorology
- 783 Gerdener, H., Kusche, J., Schulze, K., Döll, P., & Klos, A. (2023). The global land water stor-
- age data set release 2 (glws2.0) derived via assimilating grace and grace-fo data into a global
- hydrological model. Journal of Geodesy, 97, 73. https://doi.org/https://doi.org/10.1007/
- 786 s00190-023-01763-9
- 787 Getirana, A., Kumar, S., Girotto, M., & Rodell, M. (2017). Rivers and Floodplains
- as Key Components of Global Terrestrial Water Storage Variability. Geophysical Re-
- search Letters, 44(20), 10,359-10,368. https://doi.org/10.1002/2017GL074684. _eprint:
- https://onlinelibrary.wiley.com/doi/pdf/10.1002/2017GL074684
- 791 Grillakis, M. G., Koutroulis, A. G., Alexakis, D. D., Polykretis, C., & Daliakopoulos, I. N.
- 792 (2021). Regionalizing Root-Zone Soil Moisture Estimates From ESA CCI Soil Water In-
- dex Using Machine Learning and Information on Soil, Vegetation, and Climate. Water Re-
- sources Research, 57(5), e2020WR029249. https://doi.org/10.1029/2020WR029249. _eprint:
- https://onlinelibrary.wiley.com/doi/pdf/10.1029/2020WR029249
- 796 Grippa, M., Kergoat, L., Frappart, F., Araud, Q., Boone, A., de Rosnay, P., Lemoine, J.-M., Gas-
- coin, S., Balsamo, G., Ottlé, C., Decharme, B., Saux-Picart, S., & Ramillien, G. (2011). Land
- vater storage variability over West Africa estimated by Gravity Recovery and Climate Experiment
- 799 (GRACE) and land surface models. Water Resources Research, 47(5). https://doi.org/10.1029/
- 2009WR008856. _eprint: https://onlinelibrary.wiley.com/doi/pdf/10.1029/2009WR008856





- gruber, A., De Lannoy, G., Albergel, C., Al-Yaari, A., Brocca, L., Calvet, J. C., Colliander, A., Cosh,
- M., Crow, W., Dorigo, W., Draper, C., Hirschi, M., Kerr, Y., Konings, A., Lahoz, W., McColl,
- 803 K., Montzka, C., Muñoz-Sabater, J., Peng, J., Reichle, R., Richaume, P., Rüdiger, C., Scanlon,
- T., van der Schalie, R., Wigneron, J. P., & Wagner, W. (2020). Validation practices for satellite
- soil moisture retrievals: What are (the) errors? Remote Sensing of Environment, 244, 111806.
- 806 https://doi.org/10.1016/j.rse.2020.111806
- 607 Gruhier, C., de Rosnay, P., Hasenauer, S., Holmes, T., de Jeu, R., Kerr, Y., Mougin, E., Njoku, E.,
- Timouk, F., Wagner, W., & Zribi, M. (2010). Soil moisture active and passive microwave products:
- intercomparison and evaluation over a Sahelian site. Hydrology and Earth System Sciences, 14(1),
- 141-156. https://doi.org/10.5194/hess-14-141-2010. Publisher: Copernicus GmbH
- 811 Guilloteau, C., Gosset, M., Vignolles, C., Alcoba, M., Tourre, Y. M., & Lacaux, J.-P. (2014). Impacts
- of Satellite-Based Rainfall Products on Predicting Spatial Patterns of Rift Valley Fever Vectors.
- Journal of Hydrometeorology, 15(4), 1624-1635. https://doi.org/10.1175/JHM-D-13-0134.1.
- Publisher: American Meteorological Society Section: Journal of Hydrometeorology
- 815 Helman, D., Lensky, I. M., & Bonfil, D. J. (2019). Early prediction of wheat grain yield production
- from root-zone soil water content at heading using Crop RS-Met. Field Crops Research, 232, 11–23.
- https://doi.org/10.1016/j.fcr.2018.12.003
- 818 Hirschi, M., Crezee, B., Stradiotti, P., Dorigo, W., & Seneviratne, S. I. (2023). Characteris-
- ing recent drought events in the context of dry-season trends using state-of-the-art reanaly-
- sis and remote-sensing soil moisture products. EGUsphere, 1-41. https://doi.org/10.5194/
- egusphere-2023-2499. Publisher: Copernicus GmbH
- 822 IPCC (2023). Sections. In: Climate Change 2023: Synthesis Report. Contribution of Working Groups
- 823 I, II and III to the Sixth Assessment Report of the Intergovernmental Panel on Climate Change
- [Core Writing Team, H. Lee and J. Romero (eds.)]. Intergovernmental Panel on Climate Change.
- https://doi.org/10.59327/IPCC/AR6-9789291691647
- Jensen, L., Gerdener, H., Eicker, A., Kusche, J., & Fiedler, S. (2024). Observations indicate regionally
- misleading wetting and drying trends in CMIP6. npj Climate and Atmospheric Science, 7(1), 1–12.
- https://doi.org/10.1038/s41612-024-00788-x. Publisher: Nature Publishing Group
- Jung, H. C., Getirana, A., Arsenault, K. R., Kumar, S., & Maigary, I. (2019). Improving surface soil
- moisture estimates in West Africa through GRACE data assimilation. Journal of Hydrology, 575,
- 831 192-201. https://doi.org/10.1016/j.jhydrol.2019.05.042





- 832 Kerr, Y. H., Waldteufel, P., Richaume, P., Wigneron, J. P., Ferrazzoli, P., Mahmoodi, A., Al Bitar, A.,
- Cabot, F., Gruhier, C., Juglea, S. E., Leroux, D., Mialon, A., & Delwart, S. (2012). The SMOS Soil
- Moisture Retrieval Algorithm. IEEE Transactions on Geoscience and Remote Sensing, 50(5), 1384–
- 1403. https://doi.org/10.1109/TGRS.2012.2184548. Conference Name: IEEE Transactions on
- 836 Geoscience and Remote Sensing
- Koster, R. D., Dirmeyer, P. A., Guo, Z., Bonan, G., Chan, E., Cox, P., Gordon, C. T., Kanae, S.,
- Kowalczyk, E., Lawrence, D., Liu, P., Lu, C.-H., Malyshev, S., McAvaney, B., Mitchell, K., Mocko,
- D., Oki, T., Oleson, K., Pitman, A., Sud, Y. C., Taylor, C. M., Verseghy, D., Vasic, R., Xue, Y.,
- & Yamada, T. (2004). Regions of Strong Coupling Between Soil Moisture and Precipitation. Sci-
- ence, 305(5687), 1138-1140. https://doi.org/10.1126/science.1100217. Publisher: American
- Association for the Advancement of Science
- 843 Koster, R. D., Guo, Z., Yang, R., Dirmeyer, P. A., Mitchell, K., & Puma, M. J. (2009). On the Nature
- of Soil Moisture in Land Surface Models. Journal of Climate, 22(16), 4322-4335. https://doi.
- org/10.1175/2009JCLI2832.1. Publisher: American Meteorological Society Section: Journal of
- 846 Climate
- 847 Lange, S., Mengel, M., Treu, S., & Büchner, M. (2022). Isimip3a atmospheric climate input data.
- 848 https://doi.org/https://doi.org/10.48364/ISIMIP.982724
- Lawrence, D. M., Fisher, R. A., Koven, C. D., Oleson, K. W., Swenson, S. C., Bonan, G., Col-
- lier, N., Ghimire, B., van Kampenhout, L., Kennedy, D., Kluzek, E., Lawrence, P. J., Li, F.,
- Li, H., Lombardozzi, D., Riley, W. J., Sacks, W. J., Shi, M., Vertenstein, M., Wieder, W. R.,
- Xu, C., Ali, A. A., Badger, A. M., Bisht, G., van den Broeke, M., Brunke, M. A., Burns,
- S. P., Buzan, J., Clark, M., Craig, A., Dahlin, K., Drewniak, B., Fisher, J. B., Flanner, M.,
- Fox, A. M., Gentine, P., Hoffman, F., Keppel-Aleks, G., Knox, R., Kumar, S., Lenaerts, J.,
- Leung, L. R., Lipscomb, W. H., Lu, Y., Pandey, A., Pelletier, J. D., Perket, J., Randerson,
- J. T., Ricciuto, D. M., Sanderson, B. M., Slater, A., Subin, Z. M., Tang, J., Thomas, R. Q.,
- Val Martin, M., & Zeng, X. (2019). The Community Land Model Version 5: Description of
- New Features, Benchmarking, and Impact of Forcing Uncertainty. Journal of Advances in Mod-
- eling Earth Systems, 11(12), 4245-4287. https://doi.org/10.1029/2018MS001583. _eprint:
- https://onlinelibrary.wiley.com/doi/pdf/10.1029/2018MS001583
- Louvet, S., Pellarin, T., al Bitar, A., Cappelaere, B., Galle, S., Grippa, M., Gruhier, C., Kerr, Y.,
- Lebel, T., Mialon, A., Mougin, E., Quantin, G., Richaume, P., & de Rosnay, P. (2015). SMOS





- soil moisture product evaluation over West-Africa from local to regional scale. Remote Sensing of
- Environment, 156, 383-394. https://doi.org/10.1016/j.rse.2014.10.005
- 865 Molero, B., Leroux, D. J., Richaume, P., Kerr, Y. H., Merlin, O., Cosh, M. H.,
- & Bindlish, R. (2018). Multi-Timescale Analysis of the Spatial Representativeness of
- ⁸⁶⁷ In Situ Soil Moisture Data within Satellite Footprints. Journal of Geophysical Re-
- search: Atmospheres, 123(1), 3-21. https://doi.org/10.1002/2017JD027478. Leprint:
- https://onlinelibrary.wiley.com/doi/pdf/10.1002/2017JD027478
- 870 Montzka, C., Bogena, H. R., Zreda, M., Monerris, A., Morrison, R., Muddu, S., & Vereecken, H.
- 871 (2017). Validation of Spaceborne and Modelled Surface Soil Moisture Products with Cosmic-Ray
- Neutron Probes. Remote Sensing, 9(2), 103. https://doi.org/10.3390/rs9020103. Number: 2
- Publisher: Multidisciplinary Digital Publishing Institute
- Myeni, L., Moeletsi, M. E., & Clulow, A. D. (2019). Present status of soil moisture estimation over
- the African continent. Journal of Hydrology: Regional Studies, 21, 14-24. https://doi.org/10.
- 876 1016/j.ejrh.2018.11.004
- 877 Müller Schmied, H., Cáceres, D., Eisner, S., Flörke, M., Herbert, C., Niemann, C., Peiris, T. A., Popat,
- E., Portmann, F. T., Reinecke, R., Schumacher, M., Shadkam, S., Telteu, C.-E., Trautmann, T.,
- & Döll, P. (2021). The global water resources and use model WaterGAP v2.2d: model description
- and evaluation. Geoscientific Model Development, 14(2), 1037-1079. https://doi.org/10.5194/
- gmd-14-1037-2021. Publisher: Copernicus GmbH
- 882 Nerger, L. & Hiller, W. (2013). Software for ensemble-based data assimilation sys-
- tems—Implementation strategies and scalability. Computers & Geosciences, 55, 110-118. https:
- //doi.org/10.1016/j.cageo.2012.03.026
- Nicolai-Shaw, N., Hirschi, M., Mittelbach, H., & Seneviratne, S. I. (2015). Spatial representativeness
- of soil moisture using in situ, remote sensing, and land reanalysis data. Journal of Geophysical
- 887 Research: Atmospheres, 120(19), 9955-9964. https://doi.org/10.1002/2015JD023305. _eprint:
- https://onlinelibrary.wiley.com/doi/pdf/10.1002/2015JD023305
- 889 Njoku, E., Jackson, T., Lakshmi, V., Chan, T., & Nghiem, S. (2003). Soil moisture retrieval from
- 890 AMSR-E. IEEE Transactions on Geoscience and Remote Sensing, 41(2), 215-229. https://doi.
- org/10.1109/TGRS.2002.808243
- Oloruntoba, B. J., Kollet, S., Montzka, C., Vereecken, H., & Hendricks Franssen, H.-J. (2025). High-
- resolution land surface modelling over africa: the role of uncertain soil properties in combination with





- forcing temporal resolution. Hydrology and Earth System Sciences, 29(6), 1659–1683. https://doi.
- org/10.5194/hess-29-1659-2025. © Author(s) 2025. Distributed under the Creative Commons
- 896 Attribution 4.0 License.
- 997 Orlowsky, B. & Seneviratne, S. I. (2014). On the spatial representativeness of temporal dynamics
- at European weather stations. International Journal of Climatology, 34(10), 3154-3160. https:
- //doi.org/10.1002/joc.3903. _eprint: https://onlinelibrary.wiley.com/doi/pdf/10.1002/joc.3903
- 900 Palagiri, H., Sudardeva, N., & Pal, M. (2024). Application of ESACCI SM product-assimilated to a
- statistical model to assess the drought propagation for different Agro-Climatic zones of India using
- copula. International Journal of Applied Earth Observation and Geoinformation, 127, 103701.
- 903 https://doi.org/10.1016/j.jag.2024.103701
- 904 Pegram, G., Sinclair, S., Vischel, T., & Nxumalo, N. (2010). Soil moisture from satel-
- 905 lites: Daily maps over rsa for flash flood forecasting and drought monitoring. https:
- 906 //scholar.google.com/scholar_lookup?title=Soil%20moisture%20from%20satellites%
- 907 3A%20daily%20maps%20over%20RSA%20for%20flash%20flood%20forecasting%2C%20drought%
- 908 20monitoring&publication_year=2010&author=G.G.S.%20Pegram&author=S.%20Sinclair&
- author=T.%20Vischel&author=N.%20Nxumalo. Accessed: 25 October 2024
- 910 Pellarin, T., Laurent, J. P., Cappelaere, B., Decharme, B., Descroix, L., & Ramier, D. (2009a).
- 911 Hydrological modelling and associated microwave emission of a semi-arid region in South-western
- 912 Niger. Journal of Hydrology, 375(1), 262-272. https://doi.org/10.1016/j.jhydrol.2008.12.
- 913 003
- 914 Pellarin, T., Tran, T., Cohard, J.-M., Galle, S., Laurent, J.-P., de Rosnay, P., & Vischel, T. (2009b).
- 915 Soil moisture mapping over West Africa with a 30-min temporal resolution using AMSR-E ob-
- servations and a satellite-based rainfall product. Hydrology and Earth System Sciences, 13(10),
- 917 1887-1896. https://doi.org/10.5194/hess-13-1887-2009. Publisher: Copernicus GmbH
- 918 Portmann, F. T., Siebert, S., & Döll, P. (2010). MIRCA2000—Global monthly irrigated and rainfed
- crop areas around the year 2000: A new high-resolution data set for agricultural and hydrological
- modeling. Global Biogeochemical Cycles, 24(1). https://doi.org/10.1029/2008GB003435. _eprint:
- 921 https://onlinelibrary.wiley.com/doi/pdf/10.1029/2008GB003435
- 922 Raoult, N., Delorme, B., Ottlé, C., Peylin, P., Bastrikov, V., Maugis, P., & Polcher, J. (2018).
- 923 Confronting Soil Moisture Dynamics from the ORCHIDEE Land Surface Model With the ESA-CCI





- Product: Perspectives for Data Assimilation. Remote Sensing, 10(11), 1786. https://doi.org/
- 925 10.3390/rs10111786. Number: 11 Publisher: Multidisciplinary Digital Publishing Institute
- 926 Rodríguez-Iturbe, I. & Porporato, A. (2007). Ecohydrology of Water-
- 927 Controlled Ecosystems: Soil Moisture and Plant Dynamics. Cambridge
- 928 University Press. https://www.cambridge.org/de/academic/subjects/
- earth-and-environmental-science/hydrology-hydrogeology-and-water-resources/
- ecohydrology-water-controlled-ecosystems-soil-moisture-and-plant-dynamics
- 931 Ruichen, M., Jinxi, S., Bin, T., Wenjin, X., Feihe, K., Haotian, S., & Yuxin, L. (2023). Vegetation
- variation regulates soil moisture sensitivity to climate change on the Loess Plateau. Journal of
- 933 Hydrology, 617, 128763. https://doi.org/10.1016/j.jhydrol.2022.128763
- 934 Sadeghi, M., Gao, L., Ebtehaj, A., Wigneron, J.-P., Crow, W., Reager, J., & Warrick, A. (2020).
- Retrieving global surface soil moisture from GRACE satellite gravity data. Journal of Hydrology,
- 936 584, 124717. https://doi.org/10.1016/j.jhydrol.2020.124717. Publisher: Elsevier
- 937 Seneviratne, S. I., Corti, T., Davin, E. L., Hirschi, M., Jaeger, E. B., Lehner, I., Orlowsky, B., &
- Teuling, A. J. (2010). Investigating soil moisture-climate interactions in a changing climate: A
- review. Earth-Science Reviews, 99(3), 125-161. https://doi.org/10.1016/j.earscirev.2010.
- 940 02.004
- 941 Sonwa, D. J., Dieye, A., El Mzouri, E.-H., Majule, A., Mugabe, F. T., Omolo, N., Wouapi, H., Obando,
- J., & Brooks, N. (2017). Drivers of climate risk in African agriculture. Climate and Development,
- 9(5), 383–398. https://doi.org/10.1080/17565529.2016.1167659. Publisher: Taylor & Francis
- eprint: https://doi.org/10.1080/17565529.2016.1167659
- 945 Soti, V., Puech, C., Lo Seen, D., Bertran, A., Vignolles, C., Mondet, B., Dessay, N., & Tran, A. (2010).
- The potential for remote sensing and hydrologic modelling to assess the spatio-temporal dynamics
- of ponds in the Ferlo Region (Senegal). Hydrology and Earth System Sciences, 14(8), 1449–1464.
- https://doi.org/10.5194/hess-14-1449-2010. Publisher: Copernicus GmbH
- 949 Su, S. L., Singh, D. N., & Shojaei Baghini, M. (2014). A critical review of soil moisture measurement.
- 950 Measurement, 54, 92-105. https://doi.org/10.1016/j.measurement.2014.04.007
- 951 Tapley, B., Bettadpur, S., Ries, J., Thompson, P., & Watkins, M. (2004). GRACE measurements of
- mass variability in the Earth system. Science, 305(5683), 503-505. https://doi.org/10.1126/
- 953 science.1099192





- ⁹⁵⁴ Tappan, G. G., Cushing, W. M., Cotillon, S. E., Hutchinson, J. A., Pengra, B., Alfari, I., Botoni,
- E., Soulé, A., & Herrmann, S. M. (2016). Landscapes of West Africa: A Window on a Changing
- 956 World. United States Geological Survey. https://doi.org/10.5066/F7N014QZ
- 957 Tian, S., Renzullo, L. J., van Dijk, A. I. J. M., Tregoning, P., & Walker, J. P. (2019). Global joint
- assimilation of GRACE and SMOS for improved estimation of root-zone soil moisture and vegetation
- response. Hydrology and Earth System Sciences, 23(2), 1067-1081. https://doi.org/10.5194/
- hess-23-1067-2019. Publisher: Copernicus GmbH
- 961 UN Department of Economic and Social Affairs (2020). World Population Prospects: The 2020 revision
- 962 Population Division United Nations. https://population.un.org/wpp/. Accessed: 25 October
- 963 2024
- 964 Warrick, A. W. (1975). Analytical solutions to the one-dimensional linearized moisture flow equation
- for arbitrary input. Soil Science, 120(2), 79. https://journals.lww.com/soilsci/abstract/
- 966 1975/08000/analytical_solutions_to_the_one_dimensional.1.aspx
- 967 Watson, A., Miller, J., Künne, A., & Kralisch, S. (2022). Using soil-moisture drought indices to
- evaluate key indicators of agricultural drought in semi-arid Mediterranean Southern Africa. Science
- of The Total Environment, 812, 152464. https://doi.org/10.1016/j.scitotenv.2021.152464
- ⁹⁷⁰ Zeng, X. & Decker, M. (2009). Improving the numerical solution of soil moisture-based Richards
- equation for land models with a deep or shallow water table. Journal of Hydrometeorology, 10(1),
- 972 308-319. https://doi.org/10.1175/2008JHM1011.1
- 973 Zhang, P., Zheng, D., van der Velde, R., Zeng, J., Wang, X., Wang, Z., Zeng, Y., Wen, J., Li,
- 974 X., & Su, Z. (2024). Assessment of long-term multisource surface and subsurface soil moisture
- 975 products and estimate methods on the Tibetan Plateau. Journal of Hydrology, 640, 131713. https:
- 976 //doi.org/10.1016/j.jhydrol.2024.131713





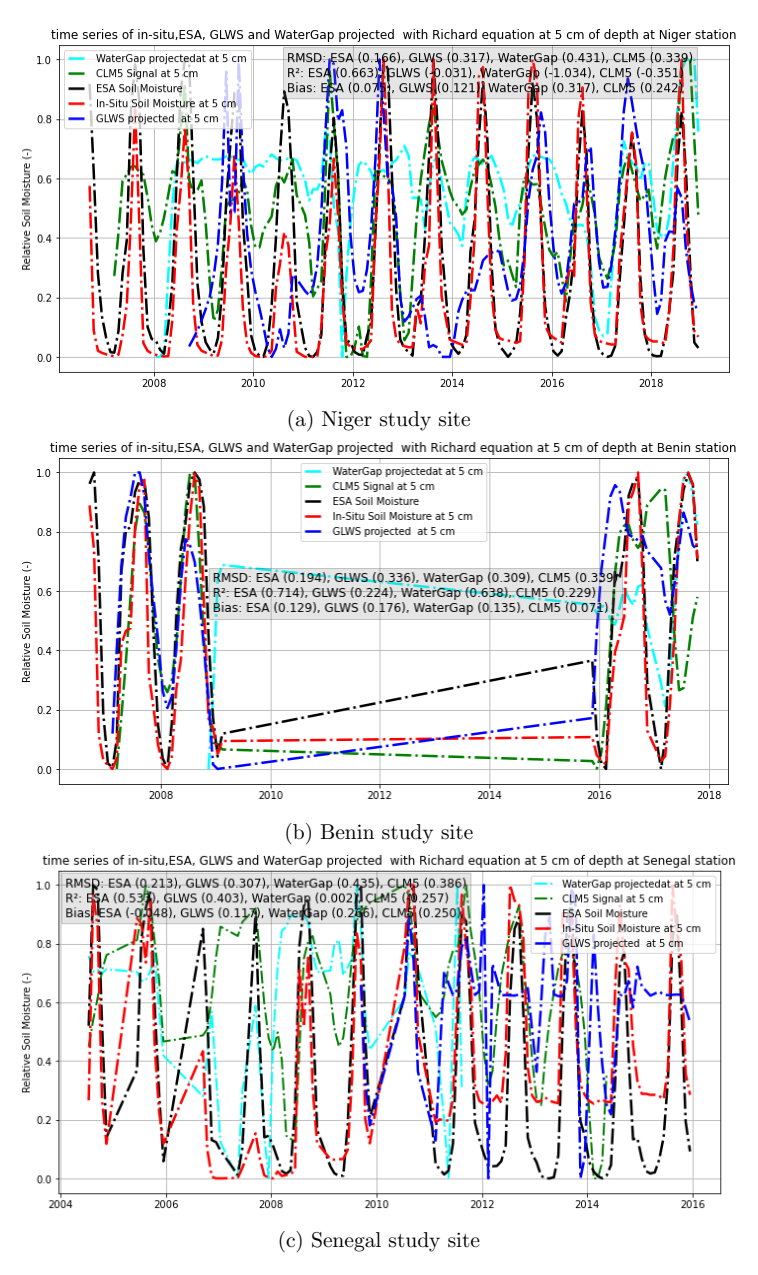


Figure 7: Soil moisture time series for in situ measurements, ESA CCI, GLWS2.0, WaterGAP, and CLM5.0 at three distinct study sites, projected at a depth of 5 cm.





• Node depth = 10 cm

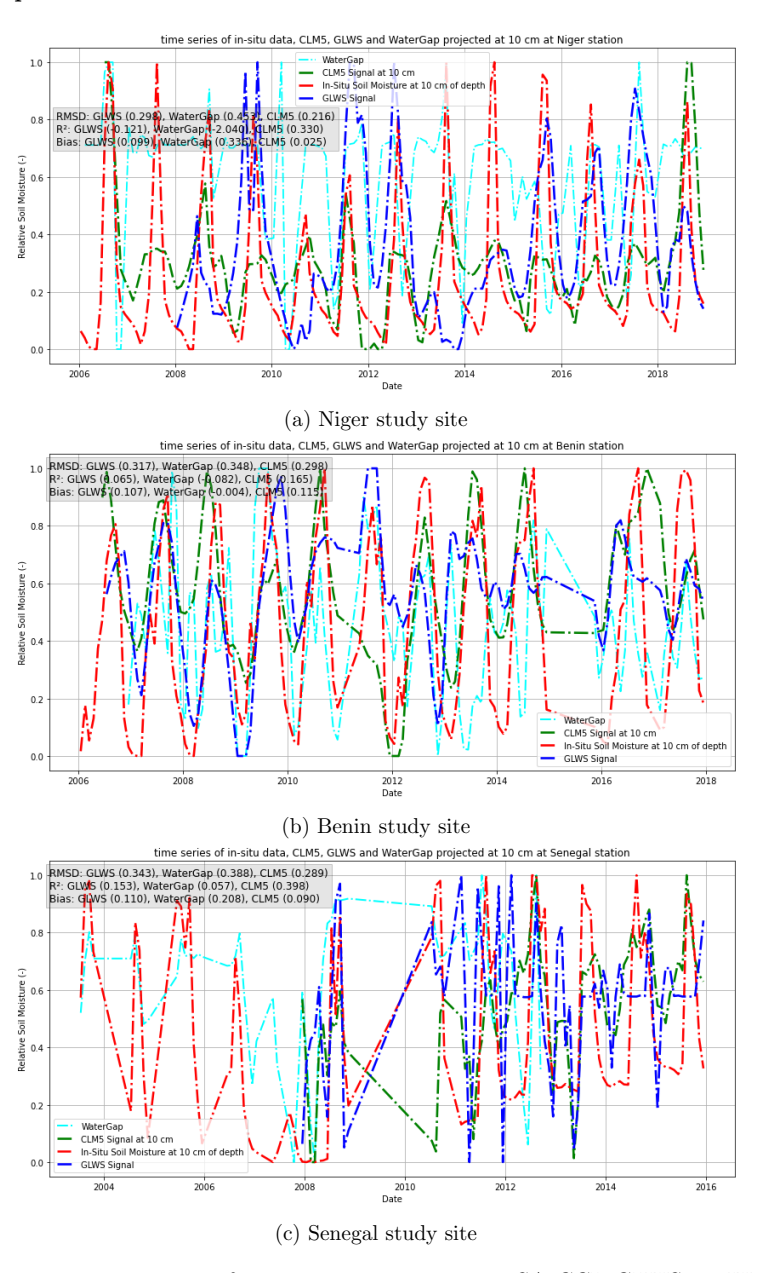
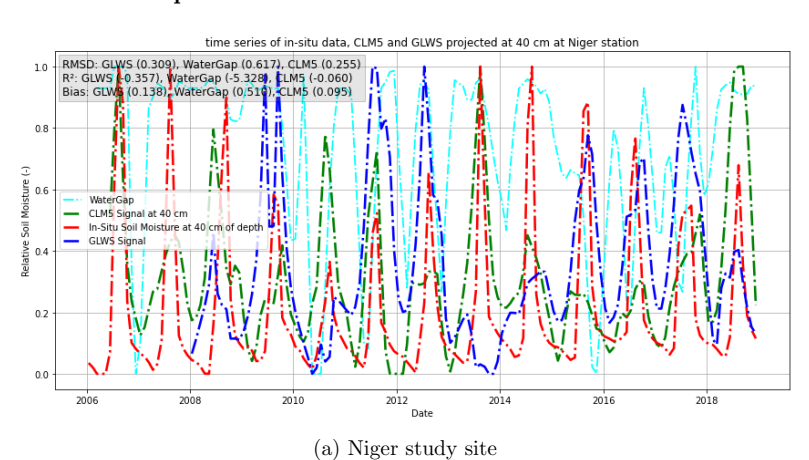


Figure 8: Soil moisture time series for in situ measurements, ESA CCI, GLWS2.0, WaterGAP, and CLM5.0 at three distinct study sites, projected at a depth of $10~\rm cm$.





• Node depth = 40 cm



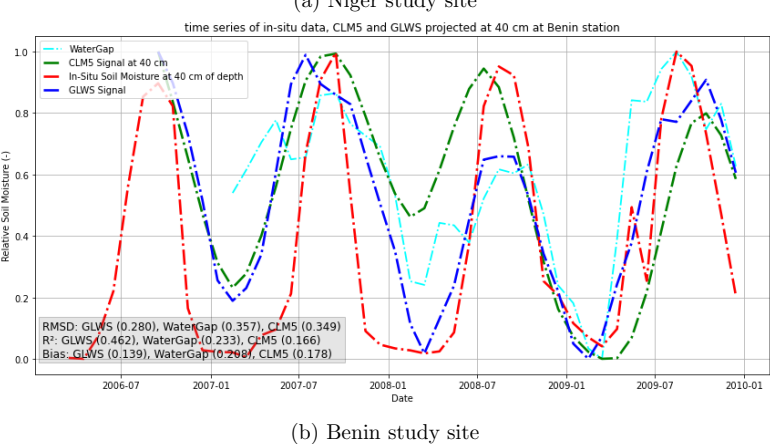


Figure 9: Soil moisture time series for in situ measurements, ESA CCI, GLWS2.0, WaterGAP, and CLM5.0 at three distinct study sites, projected at a depth of 40 cm.





• Node depth = 100 cm

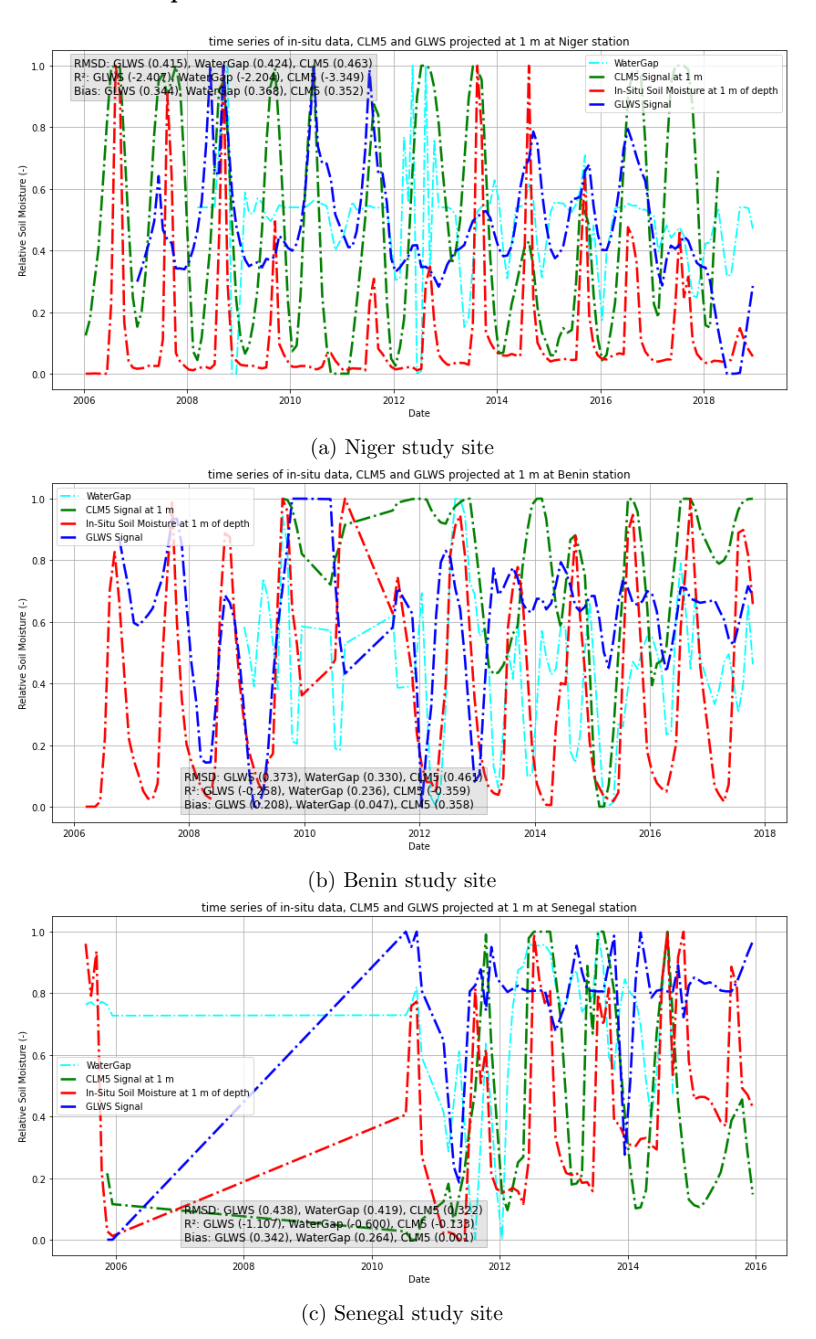


Figure 10: Soil moisture time series for in situ measurements, ESA CCI, GLWS2.0, WaterGAP, and CLM5.0 at three distinct study sites, projected at a depth of 100 cm.